The FEBS Journal

FEBS PRESS science publishing by scientists

Platelet-derived microvesicles promote endothelial progenitor cell proliferation in intimal injury by delivering TGF-β1

Jing Yan, Han Bao, Yang-Jing Fan, Zong-Lai Jiang, Ying-Xin Qi and Yue Han

Institute of Mechanobiology & Medical Engineering, School of Life Sciences & Biotechnology, Shanghai Jiao Tong University, China

Keywords
endothelial progenitor cells; intimal Injury; platelet-derived microvesicles; proliferation; transforming growth factor-β1

Correspondence
Y. Han, Institute of Mechanobiology & Medical Engineering, School of Life Science & Technology, P.O.Box 888, Shanghai Jiao Tong University, 800 Dongchuan Road, Minhang, Shanghai 200240, China
Tel: +86-21-34204863
E-mail: hanyue625@sjtu.edu.cn

(Received 12 November 2019, revised 21 February 2020, accepted 11 March 2020)

doi:10.1111/febs.15293

Intimal injury is an early stage of several cardiovascular diseases. Endothelial progenitor cells (EPCs) play a significant role in endothelial repair following vascular injury. Once the intima is damaged, EPCs are mobilized from the bone marrow to the injury site. Meanwhile, the injury to the intimal surface triggers platelet degranulation, aggregation, and adhesion to the damaged endothelium, and exposed collagen stimulates platelet to secrete platelet-derived microvesicles (PMVs). However, the role of PMVs in EPC function during this process remains unknown. In an *in vivo* study, EPCs and platelets were found to adhere to the injury site in Sprague-Dawley (SD) rat vascular injury model. *In vitro*, collagen stimulation induced the release of PMVs, and collagen-activated PMVs (ac.PMVs) significantly promoted EPC proliferation. Transforming growth factor-β1 (TGF-β1) content was increased in ac.PMVs. Activated PMVs significantly upregulated Smad3 phosphorylation in EPCs and increased Smad3 nuclear translocation from the cytoplasm. TGF-β1 knockdown ac.PMVs downregulated EPC proliferation. Recombinant TGF-β1 enhanced EPC proliferation. The TGF-β1 inhibitor SB431542 significantly repressed the intracellular signal triggered by ac.PMVs. Furthermore, the Smad3-specific phosphorylation inhibitor SIS3 effectively reversed the cell proliferation induced by ac.PMVs. Smad3 translocated to the nucleus and enhanced EPC proliferation via its downstream genes tenascin C (TNC), CDKN1A, and CDKN2A. r-TGF-β1 promoted reendothelialization and EPC proliferation *in vivo*. Our data demonstrate that activated PMVs deliver TGF-β1 from collagen-activated platelets to EPCs, which in turn activates Smad3 phosphorylation and regulates TNC, CDKN1A, and CDKN2A expression to promote EPC proliferation, suggesting that PMVs act as a key transporter and a potential therapeutic target for vascular injury.

Introduction

Endothelial progenitor cells (EPCs) are self-renewing and circulating pluripotent stem cells that can differentiate into mature endothelial cells (ECs). Asahara *et al.* [1] first reported the existence of EPCs, which positively express KDR/Flk-1, CD31, and CD34. EPCs play an important role in intimal injury caused by

Abbreviations
ac.PMVs, collagen-activated platelet-derived microvesicles; BM, bone marrow; CDKN1A, cyclin-dependent kinase inhibitor 1; CDKN2A, cyclin-dependent kinase inhibitor 2; CVD, cardiovascular disease; DAPI, diamidine-2-phenylindole dihydrochloride; Dil-ac-LDL, 1′-dioctadecyl-3,3,3′,3′-tetramethyl indocarbocyanine perchlorate-acetylated low-density lipoprotein; EC, endothelial cell; EPC, endothelial progenitor cell; GAPDH, glyceraldehyde 3-phosphate dehydrogenase; HE staining, hematoxylin–eosin staining; NTA, nanoparticle tracking analysis; qRT-PCR, quantitative real-time PCR; rTPO, recombinant thrombopoietin; SD rats, Sprague-Dawley rats; TGF-β1, transforming growth factor-β1; TNC, tenascin C.

surgery or early blood vessel disease. During this process, bone marrow (BM)-derived EPCs are recruited to the injury site [2] and are able to proliferate and differentiate into ECs to participate in intimal injury caused by cardiovascular diseases (CVD) [3-5]. In addition, it has been reported that EPCs can secrete growth factors or cytokines to participate in angiogenesis [6]. Early EPCs have a short lifespan and secrete angiogenic cytokines, while late EPCs have a stronger proliferative capacity than early EPCs [7].

Once intimal damage occurs, the subendothelial layer, which contains collagen, is exposed, and platelets are recruited and adhere to the lesion and are subsequently activated by collagen to produce large amounts of platelet-derived microvesicles (PMVs) [8,9]. PMVs are extracellular vesicles with a closed lipid bilayer membrane ranging from 100 to 1000 nm in size, and they contain proteins and microRNAs derived from platelets and mediate signal exchange between cells [10]. Increasing evidence suggests that PMVs participate in hemostasis and inflammation and are involved in the pathogenesis of CVD such as atherosclerosis [11]. However, it has also been reported that PMVs play an important role in inducing angiogenesis and stimulating post-ischemic revascularization [12]. A previous study confirmed that PMVs can be taken up by EPCs, stimulate EPCs to differentiate into ECs [13], and promote the adhesion and migration of EPCs [14]. In the past decade, abundant proteins have been shown to be the major components of PMVs.

There are high levels of transforming growth factor-β1 (TGF-β1), which is a membrane ligand that plays critical roles in the proliferation, cell growth, differentiation, and renewal of stem cells, in PMVs that contain proteins [15]. Previous studies on TGF-β1 focused more on profibrotic processes in different cell types. For example, in atrial fibrillation (AF), TGF-β1 treatment significantly promotes the expression of fibrotic biomarkers in EPCs [16]. Additionally, TGF-β1 can be released by EPCs, causing the fibrosis of other cells, such as ovarian cancer cells [17] and hepatic stellate cells [18]. However, the effects of TGF-β1 that delivered by collagen-activated PMVs (ac.PMVs) on EPCs in intimal injury are still unclear.

In this study, we established a rat model of carotid artery injury and observed the colocalization of EPCs and platelets, and we found that EPCs were enriched in PMVs. The role of PMVs in the regulation of EPC proliferation in intimal injury was investigated *in vitro* and *in vivo*, and the effect of TGF-β1 delivered by PMVs during this process was further studied. The aim of the current study was to understand how PMVs mediate EPC function to facilitate vascular repair.

Results

EPCs and platelets adhered to the intimal injury site *in vivo*

To explore the interaction between EPCs and PMVs, a carotid artery balloon injury model was established (Fig. 1A). The left common carotid artery of each rat was used as the experimental group, and the right common carotid artery was used as the autologous control. One hour after the injury, hematoxylin–eosin (HE) staining showed that platelets adhered to the carotid lumen at the intimal lesion, while the carotid lumen of the control group was smooth and flat. After 4 weeks, the intimal hyperplasia was evident, and the vessel wall was obviously thickened (Fig. 1B). Immunofluorescence staining results showed that von Willebrand factor (vWF), a marker of the ECs, was not expressed on the lumen of damaged blood vessels 1 h after intimal injury, indicating that the intimal injury model was successfully established (Fig. 1C). In the early stage of intimal injury, EPCs are recruited to the injury site, and platelets can function by releasing microvesicles (MVs). Hence, we then examined the localization of EPCs and platelets, which were identified by vWF and CD34 expression (EPCs) and CD41 expression (platelets). After intimal injury, the endothelial layer was damaged, and vWF was not expressed on vessels. Hence, the immunofluorescence staining results showed that CD34 and vWF were colocalized, indicating that EPCs adhered to the inner wall of blood vessels (Fig. 1D). Staining for CD34 and CD41 showed that they were coexpressed at the site of injury, compared to the control group (Fig. 1E).

Fig. 1. Adhesion of EPCs and PMVs in the intimal injury model. (A) Schematic diagrams of the establishment of the rat intimal injury model. (B) HE staining revealed that platelets adhered to the injury site (black arrows) 1 h after intimal injury surgery in the model group compared with the control group, and intimal hyperplasia was significant 4 weeks after surgery. (C) Intimal injury was detected by *in situ* immunofluorescence staining for vWF (red), SMA (green), and DAPI (blue). Scale bar = 200 μm. (D, E) Immunofluorescence staining was used to detect the adhesion of EPCs and platelets *in situ* compared with that in the control group. CD34, a marker of EPCs, is indicated by red fluorescence. In Figure D, green fluorescence is vWF, an EC maker. In Figure E, green fluorescence is the platelet marker CD41. Nuclei are stained blue. The white arrows indicate the adhesion sites. Scale bar = 50 μm.

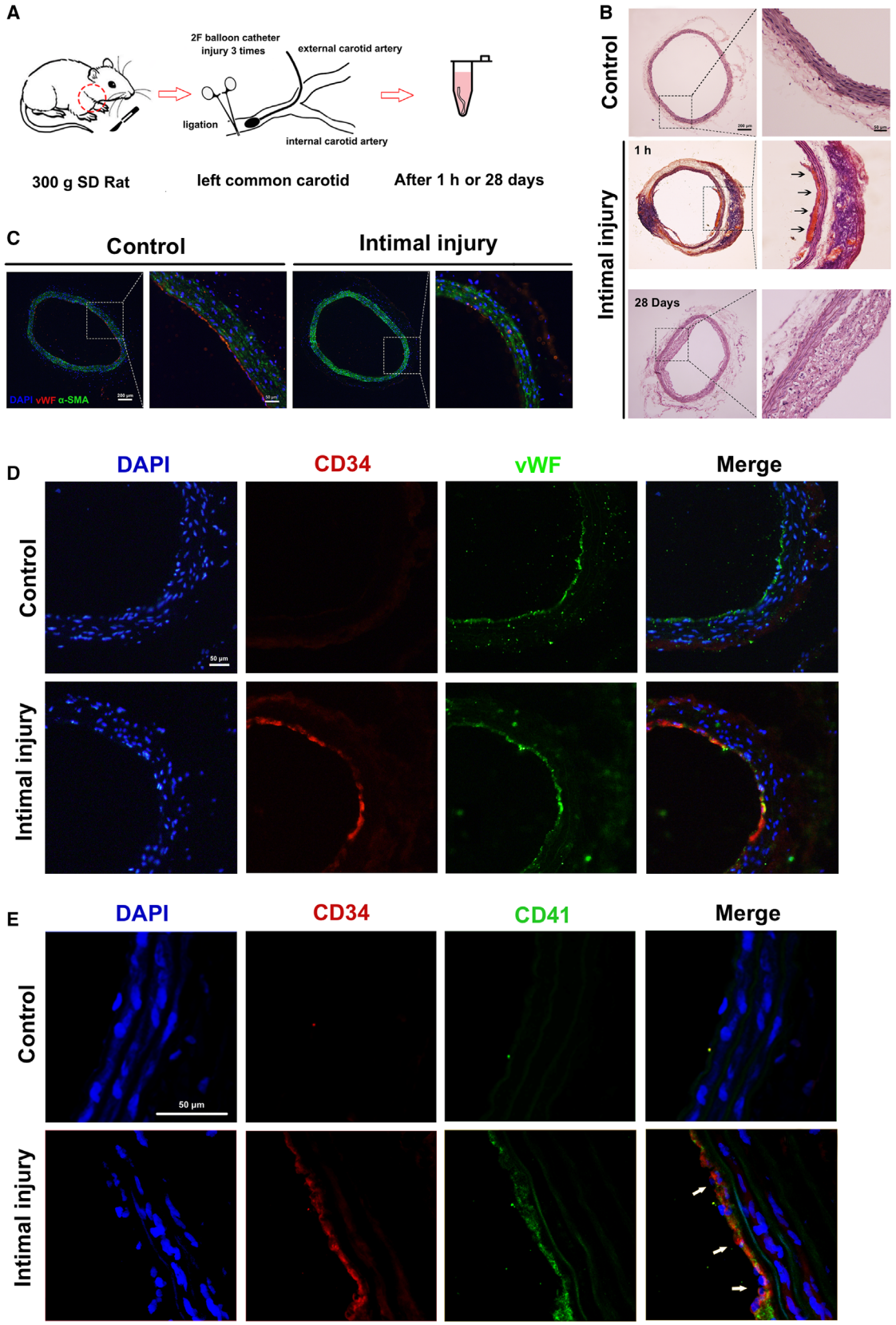
A
2F balloon catheter injury 3 times
external carotid artery
ligation
internal carotid artery
300 g SD Rat
left common carotid
After 1 h or 28 days
B
Control
Intimal injury
1 h
28 Days
C
Control
Intimal injury
DAPI vWF α-SMA
D
DAPI
CD34
vWF
Merge
Control
Intimal injury
50 μm
E
DAPI
CD34
CD41
Merge
Control
Intimal injury
50 μm

In vivo experiments suggested that carotid intimal injury caused the adhesion of EPCs and platelets. Aggregated platelets were activated by collagen exposed at the damaged intima. Hence, we hypothesized that platelets can produce large amounts of PMVs, which might have an effect on EPC function.

Collagen-activated platelet-derived microvesicles adhered to EPCs and promoted EPC proliferation

To explore the role of PMVs in EPCs, EPCs were isolated from the BM of Sprague-Dawley (SD) rats by density gradient centrifugation and identified by fluorescence microscopy. To confirm the EPC phenotype, adherent cells were stained with 1′-dioctadecyl-3,3,3′,3′-tetramethyl indocarbocyanine perchlorate-acetylated low-density lipoprotein (DiI-acLDL; red; Molecular Probes, Eugene, OR, USA) and FITC-UEA-lectin (green; Sigma, St. Louis, MO, USA), and double-positive cells were identified as EPCs (Fig. 2A). Platelets were collected from whole blood, activated with collagen (1 $\mu L \cdot mL^{-1}$; Sigma) for 1 h, and centrifuged at 20 500 ***g*** for 90 min. PMVs were isolated from the supernatant *in vitro* by density gradient centrifugation, as shown in the schematic diagrams (Fig. 2B). To investigate the adhesion of collagen-ac.PMVs to EPCs, EPCs were treated with ac.PMVs for different durations. The immunofluorescence staining results showed that PKH26-positive ac.PMVs adhered to EPCs; this adhesion increased with the prolongation of incubation time and began to show a significant increase at 1 h (Fig. 2C). More importantly, a BrdU assay confirmed that ac.PMVs significantly enhanced the proliferation of EPCs at 24 h (Fig. 2D). *In vitro* experiments indicated that collagen-ac.PMVs adhered to EPCs and significantly prompted the proliferation of EPCs.

Collagen stimulation increased the number of activated PMVs and upregulated proliferation via p-Smad3

To detect the effect of collagen on the activation of PMVs, we labeled MVs with CD41 and detected them by flow cytometry. As shown in Fig. 3A, CD41-positive MVs accounted for 90% of PMVs, and collagen stimulation increased the number of ac.PMVs compared with that in the group not treated with collagen. Meanwhile, nanoparticle tracking analysis (NTA) indicated that the size of most PMVs was between 100 and 200 nm and that the number of MVs per milliliter was significantly increased after treatment with collagen, which was consistent with the flow cytometry results (Fig. 3B). To explore the mechanisms by which ac.PMVs regulated the proliferation of EPCs, we used ingenuity pathway analysis (IPA) bioinformatics software (QIAGEN, Dusseldorf, Germany) to analyze the top upstream regulators related to cell proliferation. Among the top five upstream regulator pathways, the Smad family participated in three. Therefore, we selected Smad3, which is closely related to proliferation, for further investigation (Fig. 3C,D). EPCs were incubated with ac.PMVs *in vitro* for 1 or 24 h. The western blotting results showed that after 1 h of stimulation, the expression level of p-Smad3 in EPCs was dramatically increased and that there was no significant change in the protein level of total Smad3 (Fig. 4A). However, there was no significant change in the expression level of either p-Smad3 or total-Smad3 in EPCs treated with ac.PMVs for 24 h (Fig. 4B). In addition, ac.PMV treatment led to significant increases in the translocation of Smad3 from the cytoplasm to the nucleus in EPCs (Fig. 4C). Moreover, after ac.PMV treatment, the protein level of Smad3 was increased in the nucleus and decreased in cytosolic lysates from EPCs, which was consistent with the immunofluorescence staining results (Fig. 4D).

To verify the relationship between Smad3 phosphorylation and proliferation, a specific inhibitor of Smad3 phosphorylation, SIS3 (Selleck, Houston, TX, USA), was used [19]. The results showed that SIS3 significantly inhibited Smad3 phosphorylation (Fig. 4E) and repressed ac.PMV-induced EPC proliferation (Fig. 4F).

These results indicated that collagen stimulation significantly increased the number of ac.PMVs and upregulated EPC proliferation via Smad3 phosphorylation, which was triggered by ac.PMVs.

Activated PMVs promoted proliferation by delivering TGF-β1

We next investigated the regulator of Smad3 phosphorylation in EPCs. We hypothesized that ac.PMVs deliver key molecules to modulate EPC function. It has been reported that TGF-β1 is an upstream molecule of Smad3 and is a major cytokine that is involved in the regulation of cell growth and development. However, it is unclear whether collagen-ac.PMVs activate signaling pathways by delivering TGF-β1. Therefore, we first studied the TGF-β1 content in PMVs. Western blotting and ELISA both indicated that in the same volume, the content of TGF-β1 in ac.PMVs was significantly increased compared with that in PMVs derived from platelets that were not treated with collagen, indicating an increase

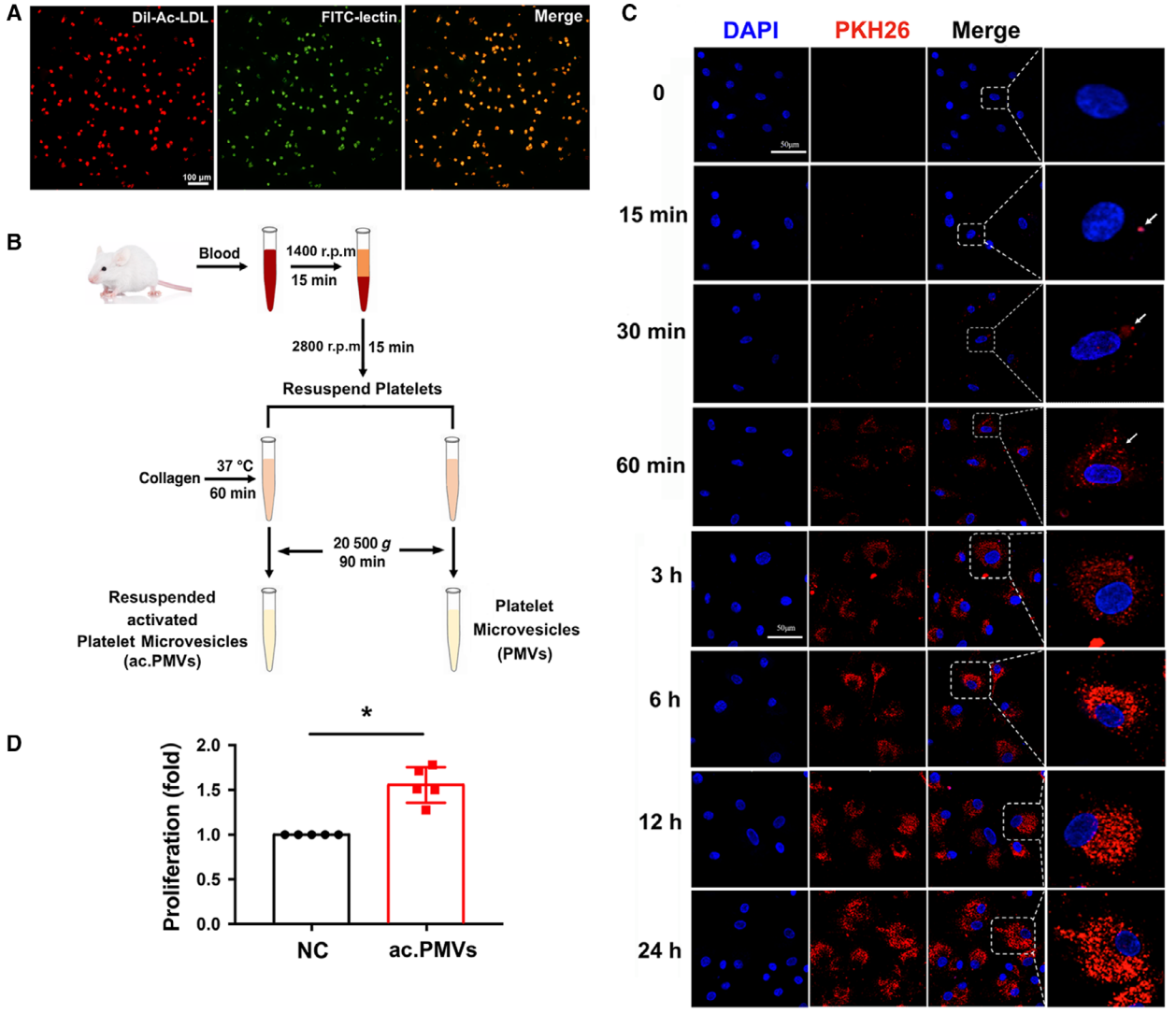

Fig. 2. Collagen-ac.PMVs adhered to EPCs *in vitro* and significantly increased the proliferation of EPCs. (A) Identification of rat BM mononuclear cell-derived EPCs. After 10 days of culture, staining for FITC-UEA-lectin (green) and DiI-acLDL (red) revealed double-positive cells that were identified as EPCs. Scale bar = 100 μm. (B) The flow chart shows the method used to obtain collagen-ac.PMVs or platelet-derived MVs. (C) ac.PMVs significantly adhered to EPCs at 1 h and continued to accumulate at 3, 6, 12, and 24 h. Red fluorescence shows the membranes of ac.PMVs, which were labeled with a PKH26 fluorescent cell linker; blue fluorescence shows the DAPI-labeled EPC nuclei. Scale bar = 50 μm. (D) The BrdU assay showed that EPC proliferation was increased by ac.PMVs ($n = 5$). *P*-values were calculated by Student's *t*-test. The values are the means ± SDs. $^*P < 0.05$.

in TGF-β1 levels due to the increased quantity of ac.PMVs (Fig. 5A,B). Furthermore, we quantified the concentration of protein in MVs. The concentration was calculated according to a standard curve, and the absorbance value of protein in PMVs was determined by the BCA Protein Assay Kit (Beyotime Biotechnology, Shanghai, China; Fig. 5C). Western blotting and ELISA analysis showed that when the same amount of total protein was loaded, the content of TGF-β1 in the ac.PMVs was increased (Fig. 5D,E), which suggested an increase in the secretion of TGF-β1 from platelets.

To investigate the mechanism by which ac.PMVs regulate EPC function and the role of TGF-β1 in this process. We used recombinant TGF-β1 protein (r-TGF-β1; Sino Biological, Beijing, China) to stimulate EPCs and detected the protein expression level of Smad3. Consistent with the results obtained after ac.PMVs stimulation, the expression of p-Smad3 in EPCs was significantly increased after treatment with

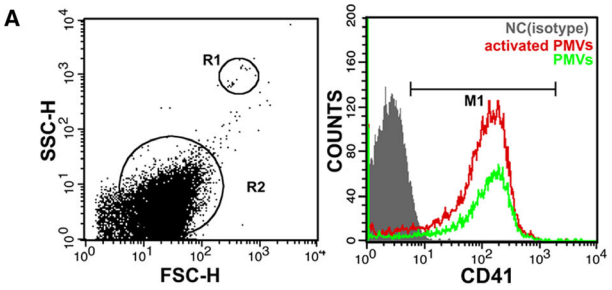

	Marker	Events	% Gated	% Total	Mean
NC(isotype)	All	20317	100.00	57.14	2.64
	M1	999	4.92	2.81	6.87
activated PMVs	All	23711	100.00	62.78	123.83
	M1	21343	90.01	56.51	137.23
PMVs	All	10545	100.00	57.27	142.34
	M1	9733	92.30	52.86	151.99

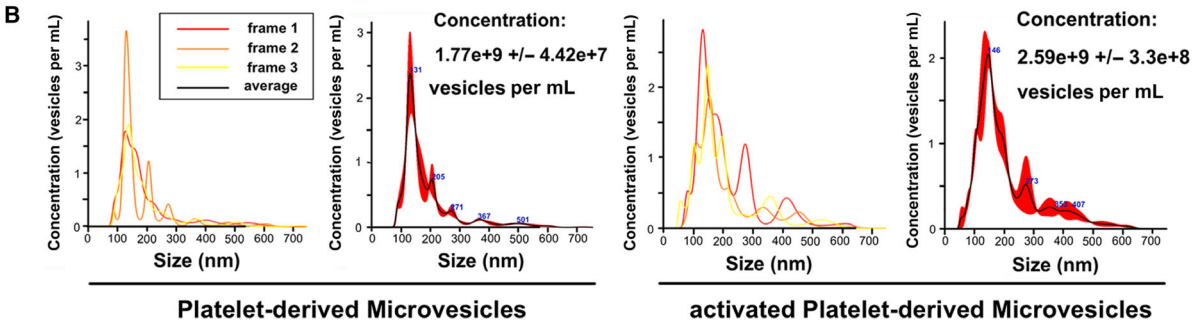

C

Top Upstream Regulators related with Cell Proliferation

Upstream Regulator	*P*-value of overlap
TGFB1	2.50E-63
FGF2	4.58E-62
SOX2	3.45E-54
CTNNB1	3.53E-52
BMP4	2.58E-49

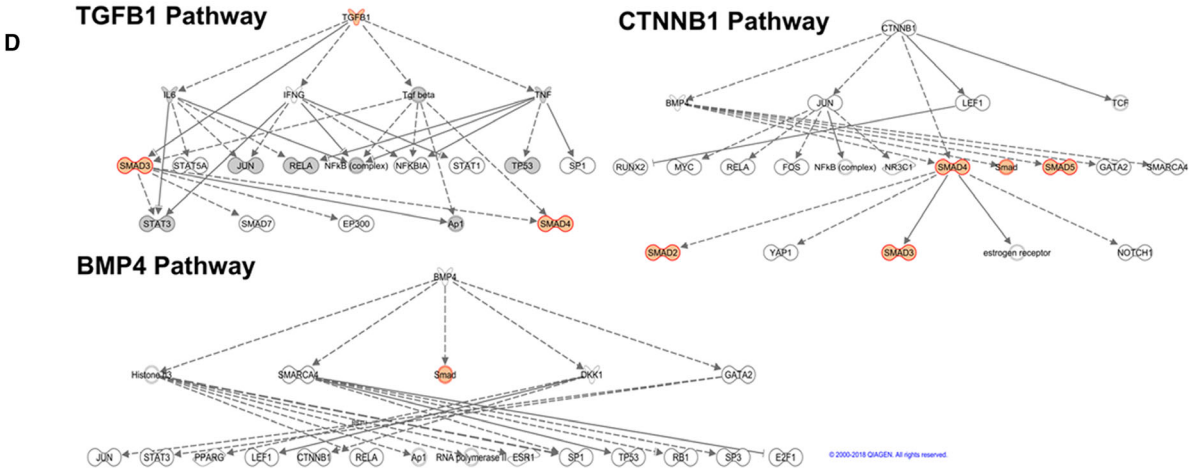

Fig. 3. Collagen stimulation increased the number of ac.PMVs. (A) Whole blood was taken from the abdominal aortas of rats, and collagen-activated or untreated PMVs (gate R1) were defined by 2.5–4.5-μm beads (gate R2). FACS analysis showed that the number of PMVs derived from platelets was increased after collagen stimulation. The red curve represents the collagen-ac.PMVs, and the green curve represents PMVs. (B) NTA was used to detect the concentration and size distribution. The results revealed that the size of the most of the two types of PMVs was between 100 and 200 nm and that the concentration of ac.PMVs was increased. (n = 3). (C, D) Upstream regulator pathways related to proliferation, as determined by IPA. (C) The top five regulators related to cell proliferation. (D) Three signaling pathway networks in which Smad family proteins are involved.

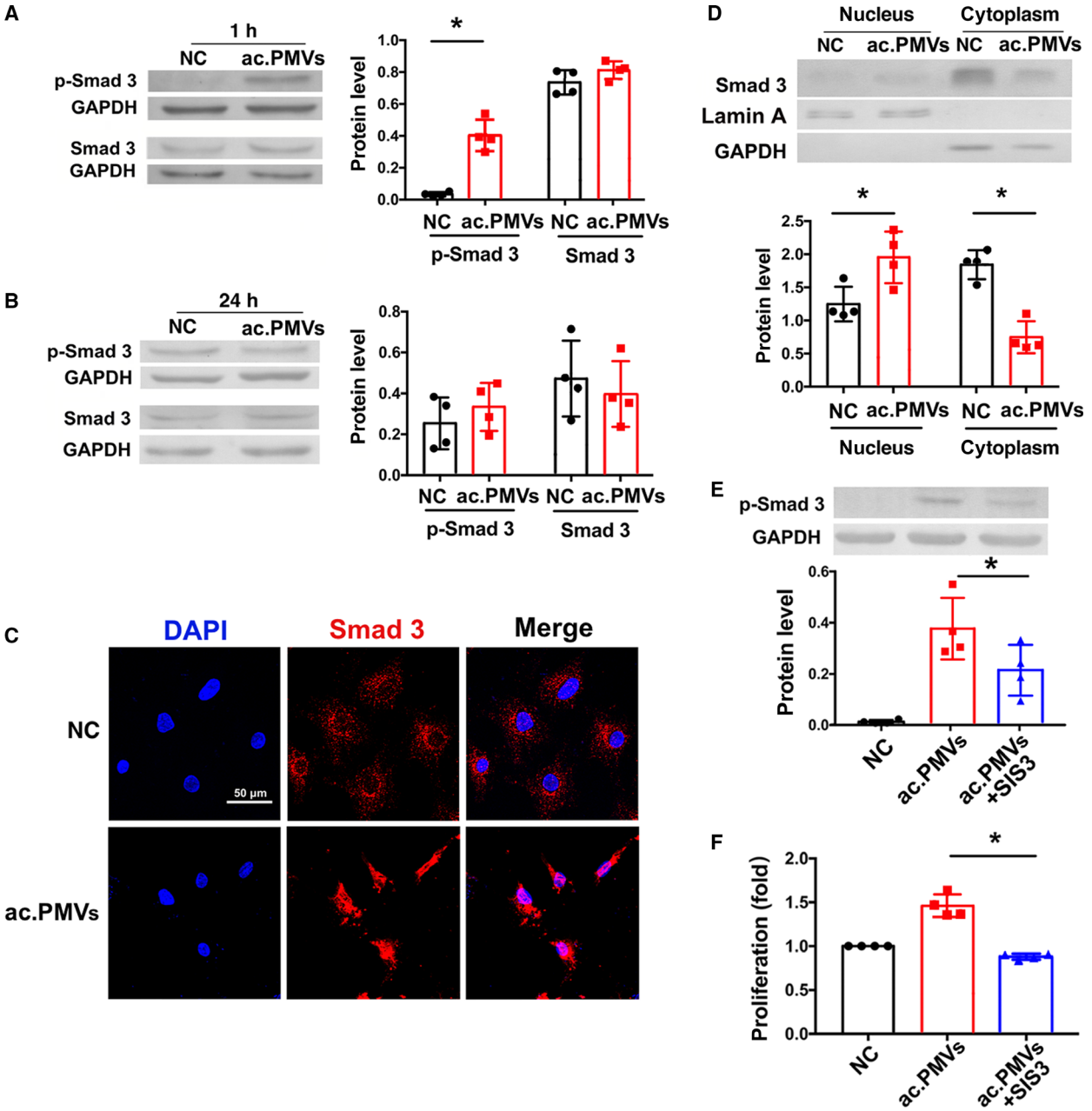

Fig. 4. Collagen-ac.PMVs triggered the Smad3 signaling pathway in EPCs. (A) Western blot analysis showed that the protein expression levels of p-Smad3 were dramatically increased in EPCs incubated with ac.PMVs for 1 h, while the total Smad3 level did not change ($n = 4$). (B) Western blotting showed that after 24 h of stimulation by ac.PMVs, p-Smad3 and total-Smad3 were not significantly changed ($n = 4$). (C) Immunofluorescence staining indicated ac.PMVs induced the translocation of Smad3 (red) from the cytoplasm to the nucleus (blue) in EPCs. Scale bar = 50 μm. (D) Western blotting results showed that Smad3 was upregulated in the nucleus after 24 h of stimulation and that the level of Smad3 in the cytoplasm was downregulated. ($n = 4$). (E, F) SIS3 inhibited the phosphorylation of Smad3 and decreased EPC proliferation. (E) Western blotting indicated that the expression level of p-Smad3 was significantly repressed in the presence of SIS3 ($n = 4$). (F) The BrdU results suggested that the proliferation of EPCs was inhibited by SIS3 ($n = 4$). SIS3 was added 1 h before stimulation with ac.PMVs. *P*-values were calculated by Student's *t*-test. The values are the means ± SDs. $^*P < 0.05$.

r-TGF-β1 for 1 h (Fig. 5F). As shown in Fig. 4D, r-TGF-β1 treatment induced the translocation of total Smad3 from the cytoplasm to the nucleus in EPCs (Fig. 5G). Moreover, EPC proliferation was significantly induced 24 h after exogenous recombinant protein stimulation (Fig. 5H).

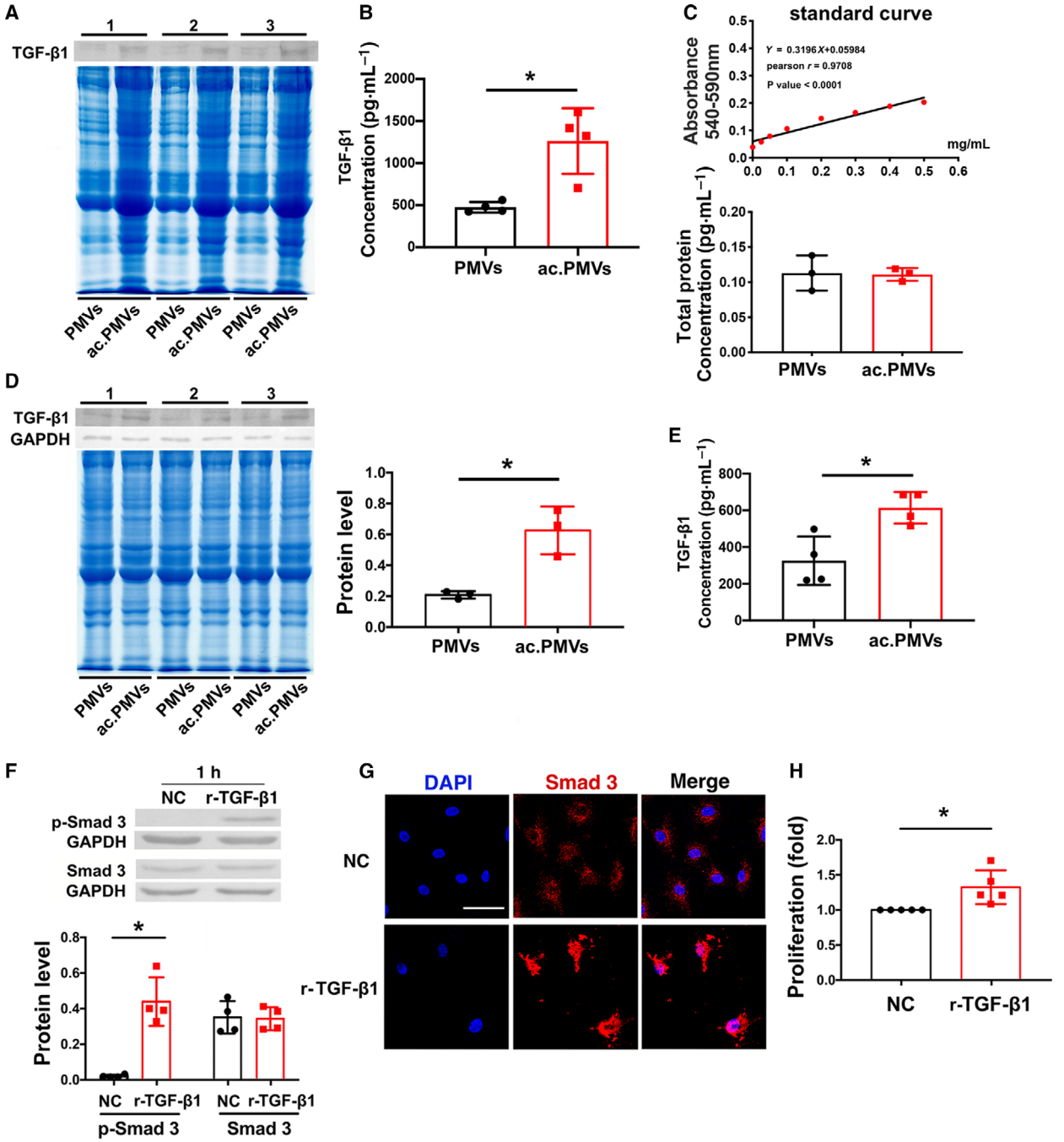

Fig. 5. Collagen stimulation increased TGF-β1 levels in ac.PMVs, and TGF-β1 promoted EPC proliferation through the Smad3 signaling pathway. (A, B) Collagen stimulation increased the TGF-β1 level in the same volume of collagen-ac.PMVs, as detected by western blotting ($n = 3$) (A) and ELISA ($n = 4$) (B). Coomassie blue staining was used to measure the amount of protein loaded. (C) Quantification of protein levels in PMVs based on a standard curve. A standard curve was drawn based on the relationship between the standard protein concentration and its absorbance (540–590 nm) according to the BCA Protein Assay Kit. A loading volume of 20 μL PMVs or collagen-ac.PMVs was used for western blotting to ensure the same protein concentration ($n = 3$). (D, E) Western blotting ($n = 3$) and ELISA ($n = 4$) revealed changes in TGF-β1 protein levels and concentrations in samples containing the same amount of total protein. Coomassie blue staining was used to indicate the amount of protein loaded. (F) EPCs were treated with r-TGF-β1 (10 ng·mL^{-1}) for 1 h, and the expression of p-Smad3 was significant, while there was no change in the total-Smad3 level ($n = 4$). (G) r-TGF-β1 treatment induced the translocation of Smad3 (red) from the cytoplasm to the nucleus (blue) in EPCs. Scale bar = 50 μm. (H) The BrdU assay results showed that the recombinant protein significantly upregulated the proliferation of EPCs ($n = 5$). *P*-values were calculated by Student's *t*-test. The values are the means ± SDs. $^*P < 0.05$.

Taken together, these data showed that collagen stimulation altered the protein content of TGF-β1 in ac.PMVs, which subsequently resulted in EPC proliferation by activating the phosphorylated Smad3 signaling pathway.

TGF-β1 specific inhibitor SB431542 inhibited EPC proliferation

To further verify the effect of TGF-β1 on EPC proliferation, SB431542, which is a specific inhibitor of the TGF-β1 signaling pathway, was used. EPCs were treated with r-TGF-β1 in the presence or absence of 10 μM SB431542 (Beyotime Biotechnology), which was added 1 h prior to recombinant protein stimulation. SB431542 significantly reversed the expression level of p-Smad3 induced by TGF-β1, but there was no significant change in the expression level of total Smad3 (Fig. 6A). After treatment with r-TGF-β1 for 24 h, SB431542 also had the same effect on repressing the phosphorylation of Smad3 (Fig. 6B). The immunofluorescence staining results showed that the addition of the TGF-β1 inhibitor blocked the nuclear translocation of Smad3 (Fig. 6C). Moreover, the BrdU results suggested that SB431542 decreased the proliferation of EPCs (Fig. 6D).

SB431542 also significantly reduced the phosphorylation of Smad3 after EPCs were stimulated with ac.PMVs for 1 h, while total Smad3 protein levels were unchanged (Fig. 7A). Similarly, immunofluorescence staining showed that the ac.PMV-stimulated nuclear translocation of Smad3 was also inhibited by SB431542 (Fig. 7B). Moreover, western blotting showed that SB431542 downregulated Smad3 protein levels in the nuclei and upregulated Smad3 protein levels in the cytosol of EPCs stimulated with ac.PMVs (Fig. 7C). Furthermore, the proliferation of EPCs induced by ac.PMVs was also inhibited by SB431542 (Fig. 7D).

In conclusion, SB431542 repressed EPC proliferation induced by ac.PMVs delivered TGF-β1 by regulating the Smad3 signaling pathway. This result verified that the transmission of TGF-β1 by ac.PMVs resulted in the proliferation of EPCs.

TGF-β1 knockdown ac.PMVs downregulated p-Smad3 activation and EPC proliferation

To further determine the role of TGF-β1 delivered by ac.PMVs in proliferation, we used a megakaryoblastic cell line, MEG-01, to produce platelets with specific TGF-β1 deletion [20]. Cells were transfected with TGF-β1 small interfering RNA (siRNA) or scrambled siRNA for 48 h and then treated with recombinant human thrombopoietin (rTPO, 100 ng·mL^{-1}; Beyotime Biotechnology) to produce platelets. We selected siRNA#2, which had good interference efficiency according to western blot analysis, for subsequent experiments (Fig. 8A). Then, we used collagen to activate platelets for 1 h and collected TGF-β1 siRNA-treated ac.PMVs and scrambled siRNA-treated ac.PMVs. ELISA confirmed that the secretion of TGF-β1 was significantly repressed in TGF-β1 siRNA-treated ac. PMVs (Fig. 8B). EPCs were stimulated with TGF-β1 siRNA-treated ac.PMVs for 1 h, and the p-Smad3 expression level was detected. Smad3 cellular localization in EPCs and EPC proliferation were examined at 24 h. The western blotting results indicated that the p-Smad3 expression level in EPCs was significantly suppressed in the group stimulated with TGF-β1 siRNA-treated ac.PMVs compared to the group stimulated with scrambled siRNA-treated ac.PMVs (Fig. 8C). Immunofluorescence staining showed that the nuclear translocation of Smad3 stimulated by ac.PMV-delivered TGF-β1 was inhibited by TGF-β1 knockdown (Fig. 8D). Furthermore, the proliferation of EPCs was downregulated (Fig. 8E).

Taken together, these results confirmed that TGF-β1 delivered by ac.PMVs led to an increase in Smad3 phosphorylation and EPC proliferation.

Smad3 promoted EPC proliferation via TNC, CDKN1A and CDKN2A

To explore how phosphorylated Smad3 regulated the proliferation of EPCs, we used IPA bioinformatics software to analyze the downstream target genes of Smad3. IPA revealed that there are 74 downstream target molecules that interact with Smad3, including 60 molecules that are associated with CVDs and seven molecules that are related to both the proliferation of stem cells and CVDs (Fig. 9A). Most of Smad3 downstream target genes are involved in atherosclerosis signaling (Fig. 9B); in addition, 52 molecules participate in cellular development, and 48 molecules are involved in cellular growth and proliferation (Fig. 9C). Among them, seven molecules involved in both stem cell proliferation and CVDs were chosen for the further investigation. To better understand which molecules are involved in EPC proliferation, the Smad3-specific inhibitor SIS3 was used to detect the mRNA expression of downstream target genes. quantitative real-time PCR (qRT-PCR) results showed that cyclin-dependent kinase inhibitors 1 and 2 (CDKN1A and CDKN2A) were significantly downregulated and that tenascin C (TNC) was upregulated by ac.PMV stimulation, while

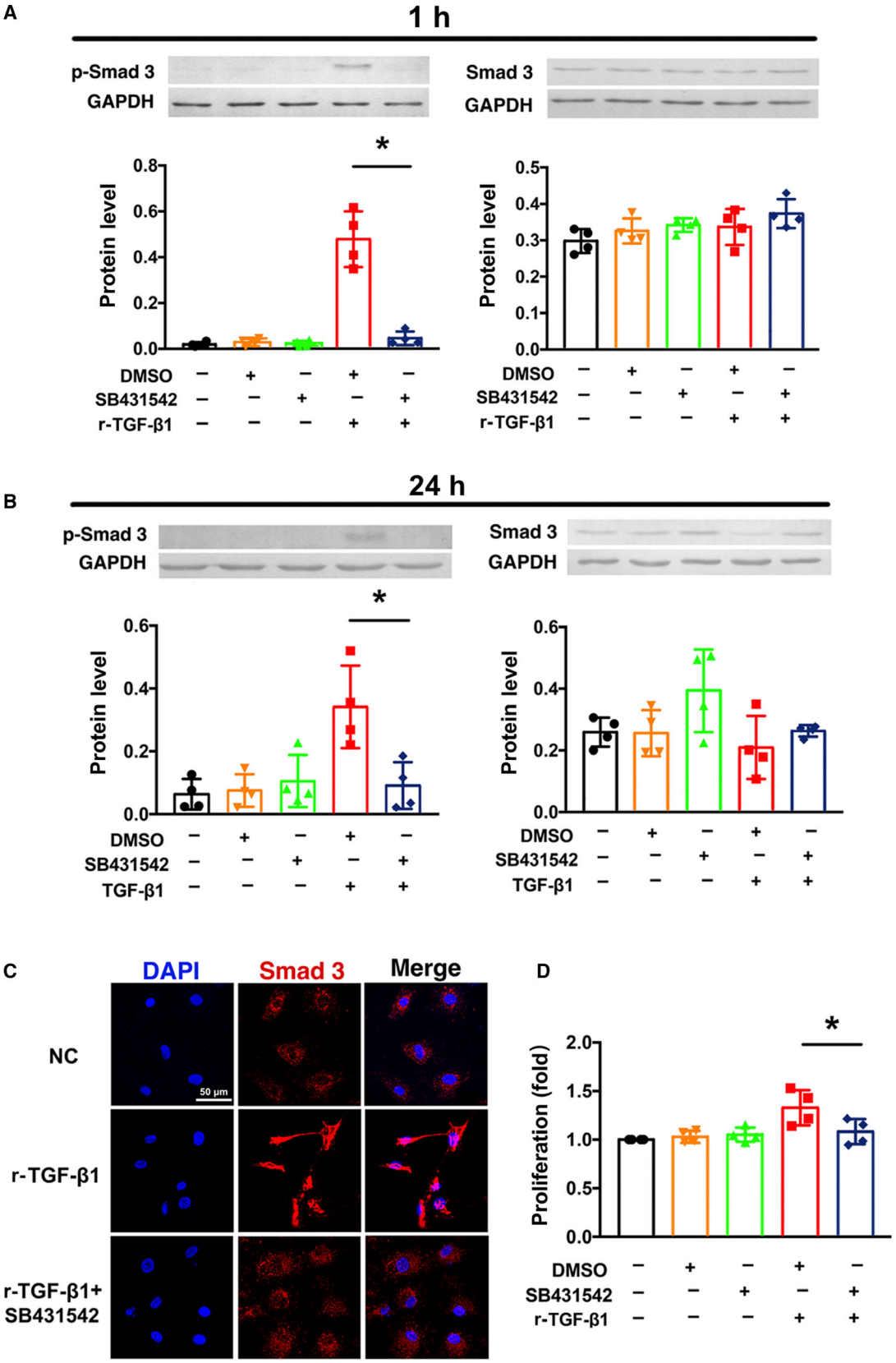
A
1 h
p-Smad 3
GAPDH
Smad 3
GAPDH
Protein level
DMSO
SB431542
r-TGF-β1
B
24 h
p-Smad 3
GAPDH
Smad 3
GAPDH
Protein level
DMSO
SB431542
TGF-β1
C
DAPI
Smad 3
Merge
NC
r-TGF-β1
r-TGF-β1+
SB431542
50 μm
D
Proliferation (fold)
DMSO
SB431542
r-TGF-β1

Fig. 6. SB431542 inhibited the proliferation of EPCs stimulated by r-TGF-β1. (A) Treatment with r-TGF-β1 for 1 h increased the phosphorylation level of Smad3, and the effect was reversed by the TGF-β1 inhibitor SB431542. The total Smad3 protein level did not change significantly. EPCs were treated with r-TGF-β1 (10 ng·mL^{-1}) for 1 h in the presence or absence of SB431542 (10 μM), which was added 1 h before ligand stimulation. DMSO, the solvent of SB431542, had no effect on EPCs ($n = 4$). (B) The expression of p-Smad3 was increased under 24 h of treatment with r-TGF-β1 (10 ng·mL^{-1}) and reversed by SB431542 (10 μM). The total-Smad3 protein level showed no change ($n = 4$). (C) Immunofluorescence staining suggested that Smad3 (red) entered the nucleus (blue) under TGF-β1 stimulation and that this was reversed by SB431542. Scale bar = 50 μm. (D) The presence of r-TGF-β1 significantly increased the proliferation of EPCs, and SB431542 inhibited the effect of recombinant protein ($n = 4$). *P*-values were calculated by Student's *t*-test. The values are the means ± SDs. $^*P < 0.05$.

the Smad3 phosphorylation inhibitor SIS3 reversed the effects of PMV stimulation (Fig. 9D).

Taken together, our results demonstrated that ac.PMV-delivered TGF-β1 induced the phosphorylation of Smad3, which subsequently regulated the downstream molecules TNC, CDKN1A, and CDKN2A and eventually induced EPC proliferation.

r-TGF-β1 enhanced intimal reendothelialization ability and EPC proliferation *in vivo*

To verify the role of TGF-β1 in EPC proliferation *in vivo*, CM-Dil-labeled EPCs (red) were instilled into and incubated in the freshly injured arteries of the animal model. r-TGF-β1 was injected via the tail vein daily for 4 days, and BrdU (Sigma) was injected via intraperitoneal injection 24 h before sacrifice. On the fourth day after the intimal injury, reendothelialization was assessed by injecting 2%, 40 mg·kg^{-1} Evans blue (Sigma) into the tail vein 30 min before sacrifice (Fig. 10A). The Evans blue dye results showed that the presence of EPCs promoted the repair of blood vessels and that the systemic injection of r-TGF-β1 significantly increased reendothelialization. When EPCs were pretreated with SB431542 for 24 h, the reendothelialization area induced by r-TGF-β1 was partially reduced *in vivo* (Fig. 10B). Furthermore, after staining with an anti-BrdU antibody, the nuclei of CM-Dil-positive cells exhibited blue [diamidine-2-phenylindole dihydrochloride (DAPI)] and green (BrdU) costaining, which indicated cell proliferation. We calculated the percentage of BrdU-positive cells to CM-Dil-positive cells based on the immunofluorescence staining. The results revealed that EPC proliferation was significantly upregulated by r-TGF-β1 and reversed by the specific inhibitor SB431542 (Fig. 10C).

The *in vivo* study results were consistent with our *in vitro* experimental results. After carotid intimal injury, local incubation with EPCs promoted the repair of the vascular intima, and the systemic injection of r-TGF-β1 significantly increased reendothelialization and EPC proliferation *in situ*.

Discussion

Endothelial dysfunction is an early critical event in CVDs [21]; the loss of monolayer ECs can cause intimal injury. Growing evidence suggests that EPCs help repair damaged intimal structure and function [22,23]. Under physiological conditions, EPCs are stored in the BM; after intimal injury, EPCs have the capacity to home to the injury site, where they proliferate and differentiate into mature ECs [24]. Previous studies have shown that treatment options based on BM-derived EPCs are promising options for treating cardiovascular disease caused by intimal injury [25].

In recent years, there have been many reports indicating that EPCs can differentiate into ECs and participate in the repair of damaged intima. For example, vascular endothelial growth factor (VEGF) or shear stress generated by blood flow through the vessel wall induces the differentiation of late EPCs into ECs phase [26,27]. Furthermore, it is also important to enhance the proliferation function of EPCs after homing. It has been reported that CD276, which is highly expressed in late EPCs, can effectively maintain cell proliferation and migration by regulating cyclin [28]. After intimal injury occurs, the increased proliferation of EPCs at the injury site implies that the number of EPCs that differentiated into ECs can also increase, which can effectively improve the efficiency of vascular repair and reduce the production of neointima. Therefore, we aimed to explore the regulation of EPC proliferation in intimal injury.

In the blood circulation, PMVs are a major component of whole blood MVs, and they have drawn increasing attention in the field of various diseases, such as coagulation disorders, rheumatoid arthritis, cancers, CVDs, and infections [29]. PMVs contain molecules such as functional enzymes [30], transcription factors [31], and nucleic acid substances [32]. They transmit information by binding with recipient cells to take part in the regulation of multiple processes. Studies have shown that, in addition to having roles in disease, PMVs can enhance cell recruitment,

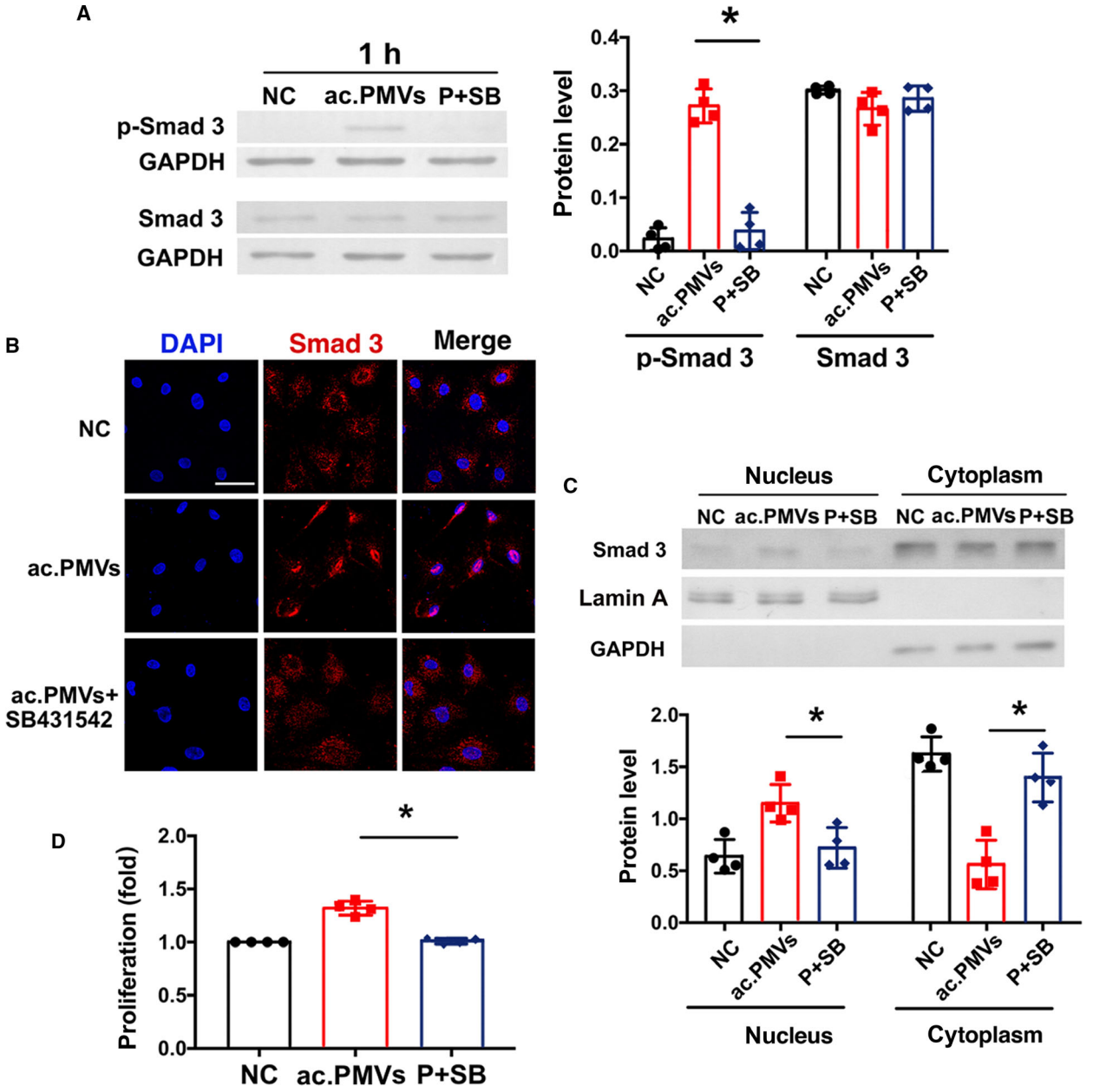

Fig. 7. SB431542 inhibited the proliferation of EPCs stimulated by collagen-ac.PMVs. (A) SB431542 inhibited the protein levels of p-Smad3 induced by ac.PMVs stimulation ($n = 4$). ac.PMV and SB (SB431542)-treated EPCs were incubated for 1 h, and SB431542 was added 1 h earlier. (B) Immunofluorescence staining indicated the Smad3 (red) nuclear translocation was reversed by SB431542 in cells. Scale bar = 50 μm. (C) Western blotting showed upregulated Smad3 protein levels in the nuclei and downregulated Smad3 protein levels in the cytosol of EPCs stimulated with ac.PMVs. The effect was reversed by SB431542 ($n = 4$). (D) The BrdU assay showed that the ac.PMV-induced EPC proliferation was blocked by the TGF-β1 inhibitor SB431542 ($n = 4$). *P*-values were calculated by Student's *t*-test. The values are the means ± SDs. $^*P < 0.05$.

differentiation, and angiogenic potential through cell membrane assimilation and incorporation during angiogenic early outgrowth. Moreover, after contact with angiogenic early outgrowth cells, PMVs activate calcium channels and AKT phosphorylation through CXCR4, which significantly increases adhesion, migration, and endothelialization for repairing intimal damage [33]. In our study, exposed collagen at the intimal injury site stimulated adherent platelets to produce large amounts of PMVs, which delivered TGF-β1 to EPCs and activated Smad3 phosphorylation in EPCs, subsequently regulating the mRNA levels of TNC,

CDKN1A, and CDKN2A and eventually enhancing the proliferation of EPCs (Fig. 11). It is worth noting that in some experimental groups, we also collected MVs derived from platelets that were untreated with collagen. These MVs served as a normal physiological control group, and EPCs incubated with untreated PMVs showed no significant change relative to EPCs incubated with the blank control PMVs (data not shown).

Transforming growth factor-β1 is a growth factor harbored by PMVs and belongs to a member of the TGF-β superfamily. It is involved in the regulation of cell growth and differentiation and is abundantly present in platelets and PMVs. Díez *et al.* [34] reported that TGF-β1 promotes the differentiation of EPCs into vascular smooth muscle-like cells by an endothelial-to-mesenchymal transition (EMT)-like process when EPCs are cocultured with vascular smooth muscle cells. However, some reports have indicated that excess TGF-β1 promotes angiogenesis [35], regulates the activity of the VEGF/VEGFR system [36], and increases the survival rate of ECs [37,38]. Previous reports have suggested that the effect of TGF-β1 on angiogenesis is diverse, but the effect of TGF-β1 delivered by PMVs on the EPC function and vascular repair is still unclear. In our current study, we were more concerned about the very early stage after intimal injury. We found EPCs immediately mobilized and adhered to the injury site 1 h after vascular injury. In this process, the landmark events are platelet adhesion, activation, and the homing of EPCs to the site of injury. The content of TGF-β1 in PMVs was significantly increased due to platelet activation by collagen. When they adhered to EPCs, ac.PMVs significantly promoted cell proliferation by transmitting TGF-β1, which played a positive role in the repair of intimal injury.

Transforming growth factor-β1 exerts its functions by phosphorylating the carboxy terminus of the activin receptors to trigger the Smad3 signaling pathway [39]. Moreover, it has also been reported that TGF-β can phosphorylate type I receptors and then phosphorylate Smad1/5 to participate in EMT together with p-Smad3 [40]. To explore the role of ac.PMVs in delivering TGF-β1, the inhibitor SB431542 was used in our study. Previous reports have shown that SB431542 can inhibit the TGF-β1 signaling pathway by limiting the function of the receptor ALK-5 [41]. In our research, we found that SB431542, as a specific inhibitor, blocked the effect of TGF-β1 delivered by ac.PMVs and significantly inhibited the proliferation of EPCs.

Smad3 is a transcription factor that is active when phosphorylated. p-Smad3 forms a complex with itself or p-Smad2, as well as Smad4, and enters the nucleus to regulate the expression of target genes. In rat BM mesenchymal stem cells (MSCs), TGF-β1 can promote the differentiation of MSCs into ECs by activating Smad3 phosphorylation in early phases; in contrast, in late phases, Smad2 inhibits the expression of VEGF and restricts cell differentiation [42]. Compared to Smad2, the effect of Smad3 on cell function is more likely to be beneficial to stem cell development through the promotion of processes such as proliferation, differentiation and tube formation. For example, GDF11 increases cell angiogenic capacity by only activating the p-Smad3 pathway [43]. Our study showed that ac.PMVs promoted EPC proliferation via p-Smad3 and facilitated the repair of intimal injury.

Tenascin C is a glycoprotein that is normally expressed in the extracellular matrix of tissue [44]. Through the variable cleavage of mRNA or activation, TNC plays an important role in regulating proliferation during wound healing [45]. CDKN1A and CDKN2A, also known as p21 and p16, are both cyclin-dependent kinase inhibitors. They inhibit cyclins, block CDK activation, and regulate cell G1/S conversion, thereby inhibiting cell proliferation. CDKN1A plays a regulatory role in binding with factors that are necessary for PCNA-dependent S-phase DNA synthesis [46]. Additionally, CDKN2A interacts with retinoblastoma (Rb) to control the G1- to S-phase transition in cells [47]. In our study, we found a positive effect of TNC and a negative effect of CDKN1A and CDKN2A as downstream molecules of p-Smad3 on EPC proliferation.

In summary, our findings identified the role of PMVs, specifically when induced by collagen, in enhancing the proliferation capacity of EPCs. After damaged, exposed collagen stimulated accumulating platelets to produce ac.PMVs, which transmitted TGF-β1 to adhered EPCs and significantly increased the intracellular p-Smad3 protein level to target TNC, CDKN1A, and CDKN2A and thus induce EPC proliferation and vascular repair. Our data provide insights into a novel process by which PMVs regulate the function of EPCs after intimal injury happens and suggest a potential therapeutic approach for the repair of injured intima.

Materials and methods

Rat carotid artery intimal injury model and reendothelialization assay

The animal care and experimental protocols in the study conformed to the recommendations in the 8th Edition of the Guide for the Care and Use of Laboratory Animals of the National Institutes of Health (NIH, revised 2011) and

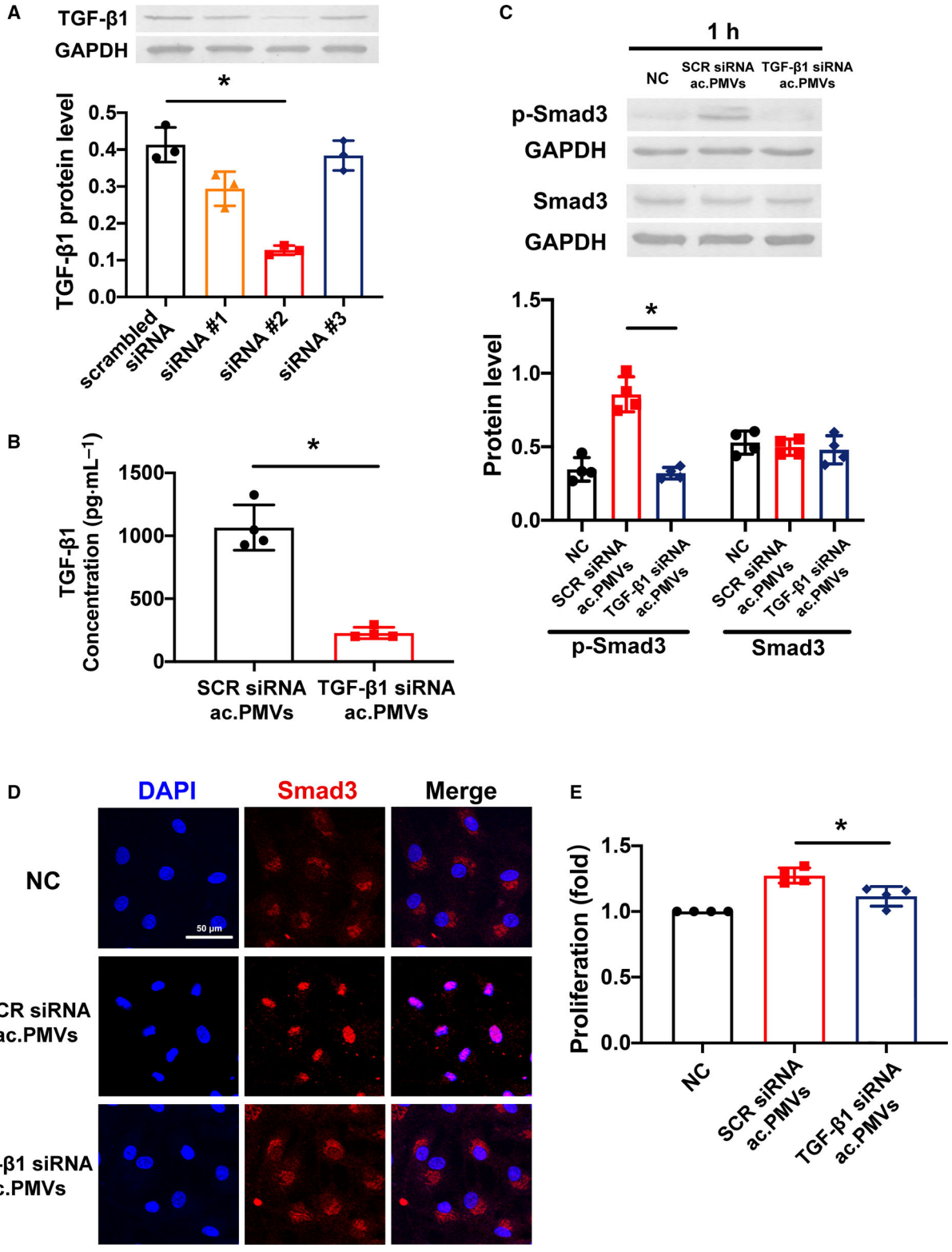
A
TGF-β1
GAPDH
*
TGF-β1 protein level
0.5
0.4
0.3
0.2
0.1
0.0
scrambled siRNA
siRNA #1
siRNA #2
siRNA #3
B
*
TGF-β1 Concentration (pg·mL⁻¹)
1500
1000
500
0
SCR siRNA ac.PMVs
TGF-β1 siRNA ac.PMVs
C
1 h
NC
SCR siRNA ac.PMVs
TGF-β1 siRNA ac.PMVs
p-Smad3
GAPDH
Smad3
GAPDH
*
Protein level
1.5
1.0
0.5
0.0
NC
SCR siRNA ac.PMVs
TGF-β1 siRNA ac.PMVs
p-Smad3
Smad3
D
DAPI
Smad3
Merge
NC
50 μm
SCR siRNA ac.PMVs
TGF-β1 siRNA ac.PMVs
E
*
Proliferation (fold)
1.5
1.0
0.5
0.0
NC
SCR siRNA ac.PMVs
TGF-β1 siRNA ac.PMVs

Fig. 8. TGF-β1 knockdown collagen-ac.PMVs downregulated EPC proliferation compared with ac.PMVs. (A) The MEG-01 cell line was transfected with siRNA, and the TGF-β1 protein level was significantly decreased by siRNA #2 after 48 h ($n = 3$). (B) The TGF-β1 concentration in MEG-01-derived ac.PMVs was significantly downregulated by siRNA, as detected by ELISA ($n = 4$). (C) Treatment with MEG-01-derived ac.PMVs or TGF-β1 siRNA-treated ac.PMVs for 1 h increased the phosphorylation level of Smad3, and this effect was reversed by TGF-β1 knockdown. The total Smad3 protein level did not change significantly ($n = 4$). (D) Immunofluorescence staining suggested that the nuclear translocation of Smad3 (red) stimulated by ac.PMV-delivered TGF-β1 was reversed by TGF-β1 knockdown. Scale bar = 50 μm. (E) ac.PMVs promoted EPC proliferation, and this effect was inhibited in the absence of TGF-β1 ($n = 4$). *P*-values were calculated by Student's *t*-test. The values are the means ± SDs. $^*P < 0.05$.

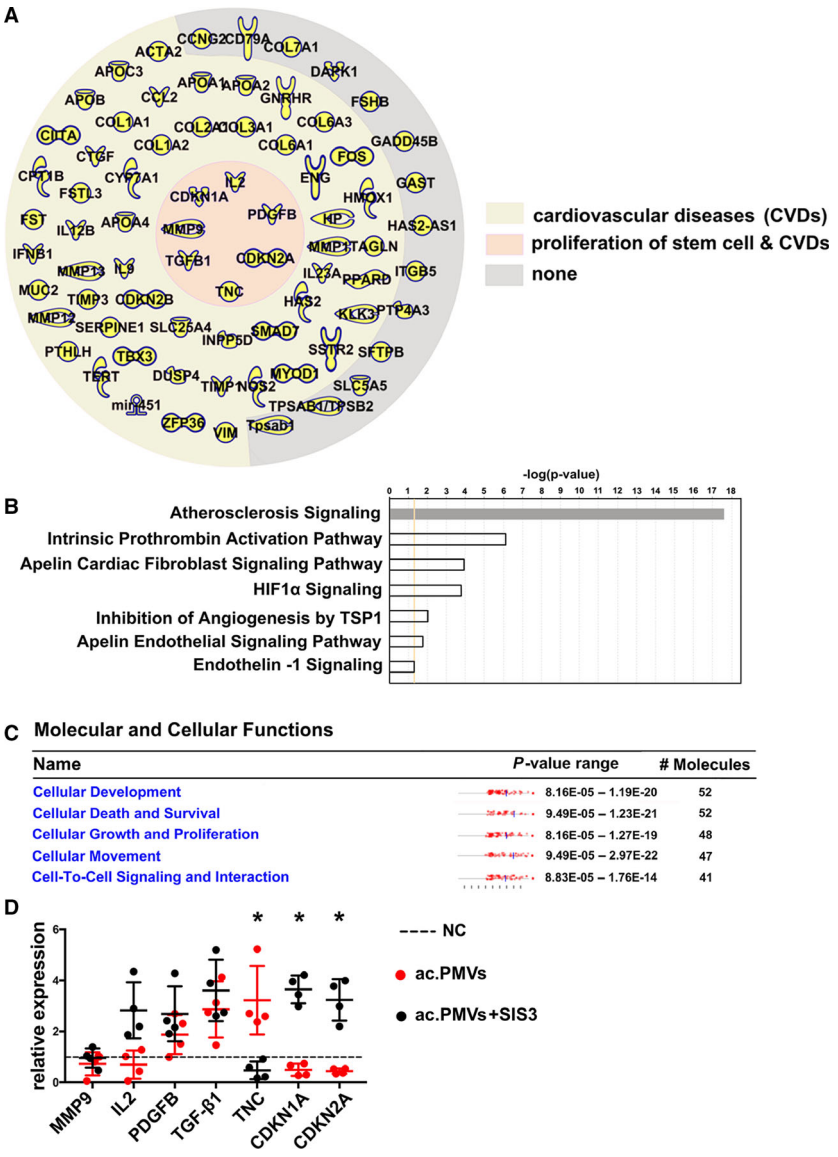

Fig. 9. ac.PMVs enhanced EPC proliferation via TNC, CDKN1A, and CDKN2A. (A) The putative target genes of Smad3 were predicted with IPA software. A total of 74 downstream target molecules that directly interact with Smad3 were identified by IPA. Sixty target molecules associated with CVDs are shown in the yellow region. The green region in the center is the seven target molecules related to both cell proliferation and CVDs. (B) IPA software analysis revealed that a large number of downstream molecules of Smad3 are involved in the atherosclerosis signaling pathway. (C) Seventy-four downstream molecules were analyzed by IPA software; 52 of them participated in cellular development; and 48 participated in cellular growth and proliferation. (D) Seven predicted downstream molecules of Smad3 in EPCs were assessed by qRT-PCR after 24 h stimulation with collagen-ac.PMVs or with both ac.PMVs and SIS3 ($n = 4$). The results showed that CDKN1A and CDKN2A were significantly downregulated and that TNC was upregulated by ac.PMV stimulation, while the Smad3 phosphorylation inhibitor SIS3 reversed the effects of ac.PMV stimulation. Column scatter showing the fold change relative to the control. *P*-values were calculated by Student's *t*-test. The values are the means ± SDs. $^*P < 0.05$.

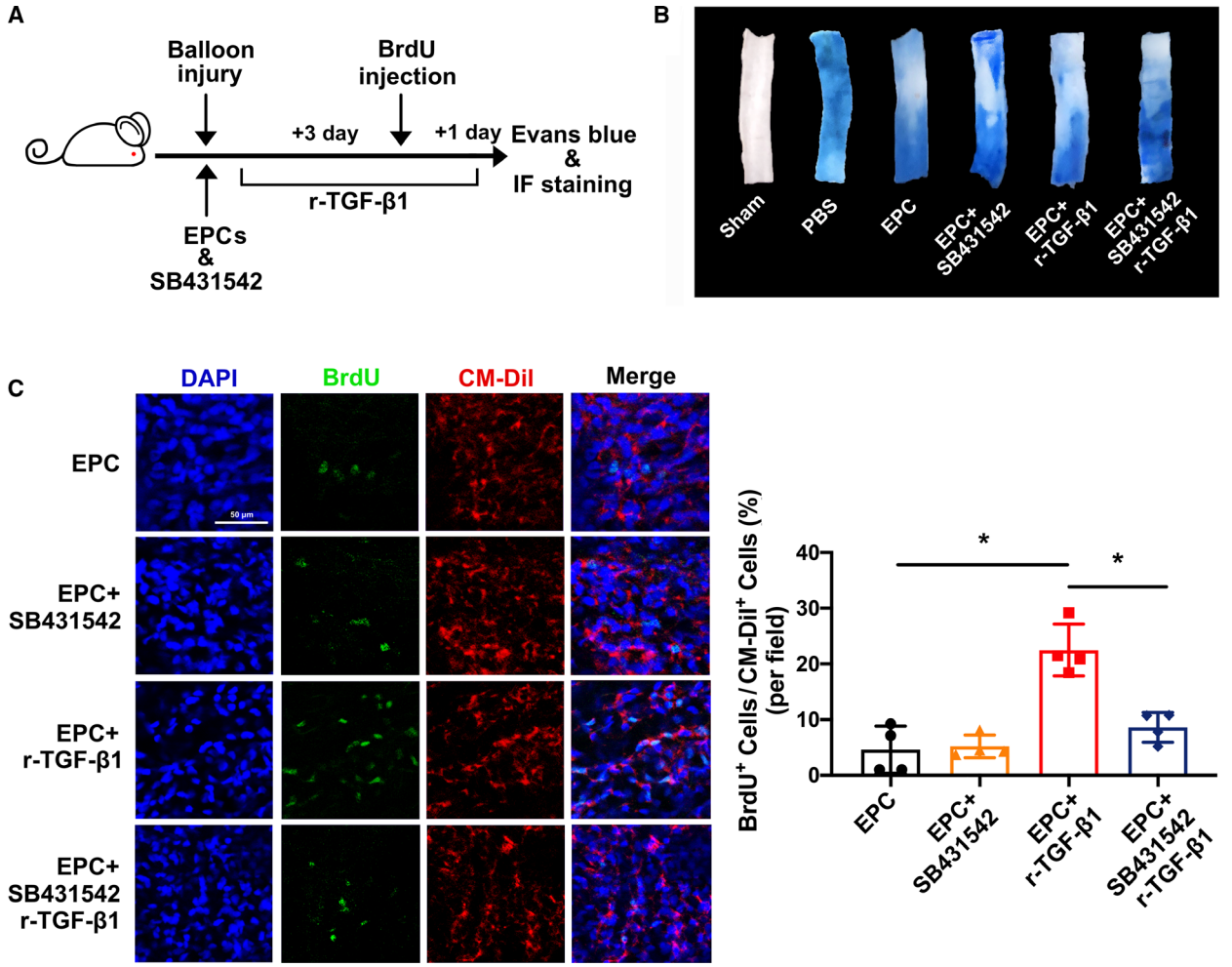

Fig. 10. r-TGF-β1 promoted vascular repair and EPC proliferation *in vivo*. (A) A flow diagram of the experimental animal protocol. (B) EPCs and r-TGF-β1 injection (10 $\mu g \cdot kg^{-1} \cdot day^{-1}$) promoted pretreated the reendothelialization of the injury site, and pretreated with SB431542 decreased reendothelialization area which detected by Evans blue staining. The blue area represents the damaged area, and the white area represents the repaired area. (C) Representative microscopy images revealed that EPC proliferation was significantly upregulated by r-TGF-β1 and reversed by the specific inhibitor SB431542. EPCs were labeled with CM-DiI (red), and proliferating cells showed double staining for BrdU (green) and DAPI (blue). The number of BrdU-positive cells to CM-DiI-positive cells is shown as a percentage ($n = 4$). Scale bar = 50 μm. *P*-values were calculated by Student's *t*-test. The values are the means ± SDs. $^*P < 0.05$.

were in accordance with the Animal Management Rules of China (Documentation 55, 2001, Ministry of Health, China), and the study was approved by the Animal Research Committee of Shanghai Jiao Tong University.

Sprague-Dawley rats were anesthetized with isoflurane, and the carotid blood vessels were exposed under a dissecting microscope. After the bifurcation above the common carotid artery was found, the occipital artery, the internal carotid artery, the thyroid artery, and the external carotid artery were sequentially ligated using a surgical suture. A hemostat was used to clamp the proximal common carotid artery. A small opening was made in the blood vessel from the proximal end of the thyroid artery and a balloon inserted (2F, 0.67 mm; Edwards Lifesciences, Irvine, CA, USA), and the inner membrane was damaged three times by rotary motion. For the BrdU *in vivo* and reendothelialization assay, EPCs were pretreated with or without SB431542 (10 μM) 24 h before surgery. EPCs (1×10^6) were labeled with CM-DiI (1 μM; YEASEN, Shanghai, China) for 5 min at 37 °C. Then, the cells were resuspended in 200 μL PBS. The cell suspension was instilled into and incubated with the freshly injured arterial bed for 25–30 min [48,49]. Recombinant TGF-β1 (10 $\mu g \cdot kg^{-1} \cdot day^{-1}$) was injected via the tail vein 3 h after intimal injury for 4 days. The postoperative rats were housed in the experimental animal center. Carotid blood vessels were collected 1 h, 4 days, or 4 weeks after the surgery for frozen sectioning and morphological staining.

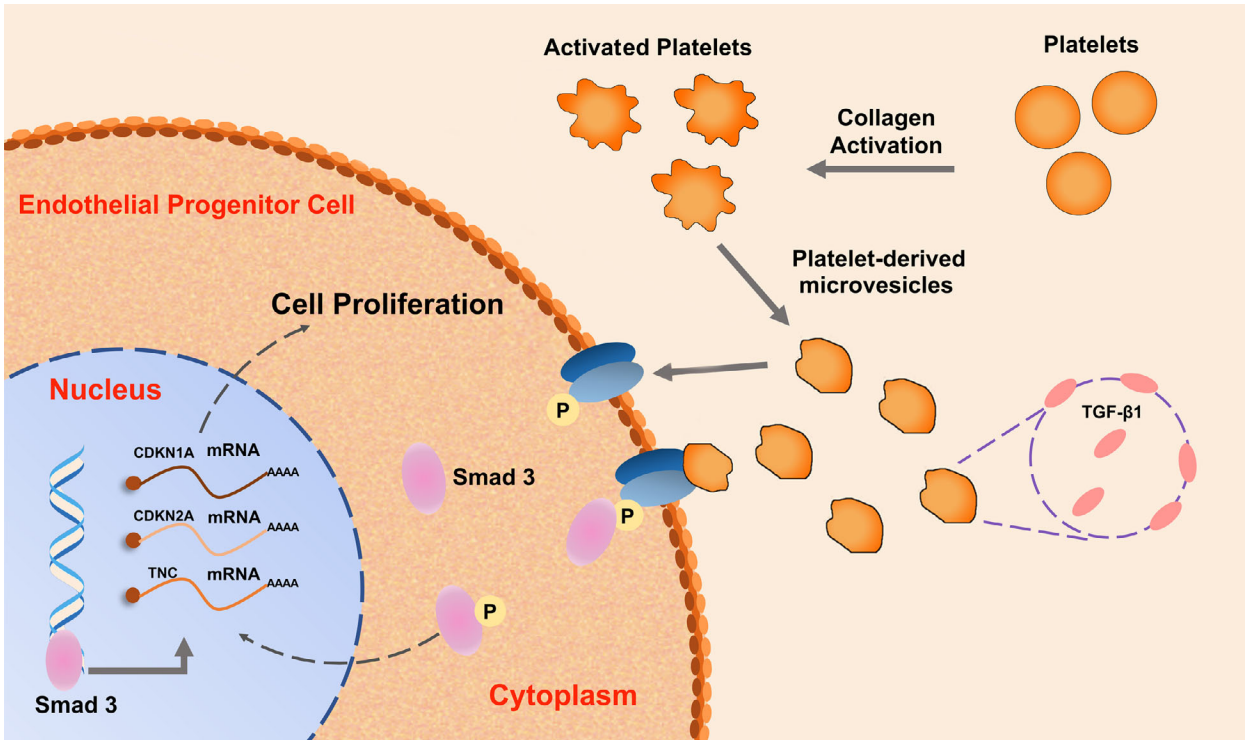

Fig. 11. The schematic depicts the role of ac.PMVs-delivered TGF-β1 in EPC proliferation during intimal injury. Exposed collagen at the intimal injury site stimulates the adherent platelets to produce a large amount of ac.PMVs, activates Smad3 phosphorylation by translocating TGF-β1 to EPCs, regulates the expression levels of TNC, CDKN1A, and CDKN2A, and eventually promotes the proliferation of EPCs.

Reendothelialization was assessed by injecting 2%, 40 mg·kg^{-1} Evans blue into the tail vein 30 min before sacrifice on the fourth day after intimal injury. The left common carotid arteries were collected from the carotid bifurcation, incised longitudinally, and photographed with a digital camera. The reendothelialized areas were defined macroscopically as those areas not stained by the Evans blue dye and quantified with IMAGEJ software (National Institutes of Health, Bethesda, MD, USA).

For frozen sections, carotid blood vessels were fixed in 4% paraformaldehyde for 24 h and dehydrated in 30% sucrose solution for 24 h. Then, frozen sections with a thickness of 10 μm were produced and stored at −20°C.

Isolation, cultivation, and characterization of EPCs

Endothelial progenitor cells were cultured from the BM of SD rats [50,51]. Briefly, the femur and tibia were removed from male SD rats (180–200 g), and all surrounding connective tissue and muscle were removed. The ends of the bones were cut, and BM was collected by irrigation with PBS. BM-derived mononuclear cells were isolated by density gradient centrifugation with Histopaque-1083 (Sigma) and cultured in six-well plates coated with 0.1% gelatin in endothelial growth medium-2 (EGM-2; Lonza, Walkersville, MD, USA) supplemented with FBS, VEGF, fibroblast growth factor-B, epidermal growth factor, hydrocortisone, R3 insulin-like growth factor-1 (R3-IGF-1), ascorbic acid, gentamicin, and amphotericin-B (GA-1000; Lonza). After 4 days, nonadherent cells were discarded and a fresh culture medium was added. The media were subsequently changed every 3 days.

Endothelial progenitor cells were identified by the classical method [1]. Adherent cells cultured for 10 days were incubated with 1′-dioctadecyl-3,3,3′,3′-tetramethyl indocarbocyanine perchlorate-acetylated low-density lipoprotein (DiI-ac-LDL) for 4 h, fixed in 4% paraformaldehyde, and counterstained with 10 μg·mL^{-1} fluorescein isothiocyanate (FITC)-labeled lectin. Cells that were positive for both DiI-ac-LDL and FITC-labeled lectin were identified as EPCs. Fluorescence images were taken using a fluorescence microscope (IX-71; Olympus, Tokyo, Japan). The methods have also been described previously [52].

Preparation of PMVs

Whole blood was collected from the abdominal aortas of anesthetized rats into syringes containing 100 μL·mL^{-1} anticoagulant (2.94% sodium citrate, 0.1 g·mL^{-1} PGE1, and 1 U·mL^{-1} apyrase), and the platelet-rich plasma was obtained by centrifugation at 600 ***g*** for 15 min. Platelets

were prepared from platelet-rich plasma by centrifugation at 2000 ***g***. for 15 min. After the platelets were collected, the remaining platelet-poor plasma was centrifuged at 20 500 ***g*** for 90 min to obtain circulating PMVs. The platelets were resuspended in modified Tyrode's solution [12 mM $NaHCO_3$, 138 mM NaCl, 5.5 mM glucose, 2.9 mM KCl, 2 mM $MgCl_2$, 0.42 mM NaH_2PO_4, and 10 mM 4-(2-hydroxyethyl)-1-piperazineethanesulfonic acid (pH 7.4)]. Resuspended platelets were activated with 1 $\mu L \cdot mL^{-1}$ collagen for 1 h and then centrifuged at 2000 ***g***. for 15 min. ac.PMVs were collected from the remaining supernatant, which was centrifuged at 20 500 ***g*** for 90 min [53].

In the present study, cells treated with collagen-ac.PMVs were used as the experimental group, and cells treated with blank medium were used as the control group (NC).

MEG-01 cells (Aolushengwu Biomart, Shanghai, China) were grown in suspension in RPMI 1640 (Gibco, Grand Island, NY, USA) with 10% FBS. MEG-01 cells were transfected with scrambled siRNA or TGF-β1-specific siRNA for 48 h and then stimulated with rTPO (100 $ng \cdot mL^{-1}$) for 48 h to produce platelets. Preparations were centrifuged at 300 ***g***. for 5 min to remove cells and then centrifuged at 2000 ***g***. for 15 min to collect platelets. The platelets were resuspended and activated with collagen as described before, and eventually, scrambled siRNA-treated ac.PMVs and TGF-β1 siRNA-treated ac.PMVs were obtained.

Small interfering RNA transfection

For the RNA interference experiment, MEG-01 was transfected with TGF-β1 siRNA or negative control siRNA (GenePharma, Shanghai, China) for 48 h with Lipofectamine 2000 in Opti-MEM (both from Thermo Fisher Scientific, Waltham, MA, USA) according to the manufacturer's instructions. The sequences of the siRNA oligos were as follows:

siRNA#1: GCGUGCUAAUGGUGGAAACTT (F), GUUUCCACCAUUAGCACGCTT (R)

siRNA#2: GACUCGCCAGAGUGGUUAUTT (F), AUAACCACUCUGGCGAGUCTT (R)

siRNA#3: CCACCAUUCAUGGCAUGAATT (F), UUCAUGCCAUGAAUGGUGGTT (R).

Flow cytometry and nanoparticle tracking analysis

Flow cytometry was used to analyze the proportion of PMVs in MVs. MVs were labeled with FITC-conjugated anti-rat CD41, a platelet-specific marker (1 : 100; Abcam, Cambridge, UK) for 1 h and then loaded into a flow cytometry column (FACSCalibur TM; BD Biosciences, San Jose, CA, USA). MVs that were positive for CD41 were considered MVs derived from platelet.

Nanoparticle tracking analysis [54] was used to analyze the number of PMVs activated by collagen. The obtained PMVs were diluted with PBS. The suspensions were equally loaded into the NanoSight module (NanoSight NS300; Malvern Panalytical, London, UK) for measurement. The module was washed with PBS after each measurement. A 600 μL dilution from each group was used to detect the concentration and size of vesicles.

Stimulation of EPCs with ac.PMVs, recombinant TGF-β1, SB431542, and SIS3

Platelet-derived microvesicles were quantified with BD Trucount Tubes (20 000/mL) by flow cytometry. EPCs were incubated with ac.PMVs (10^9/mL) for up to 1 or 24 h at 37 °C with 5% CO_2. In the inhibition experiments, EPCs were treated with recombinant TGF-β1 (10 $ng \cdot mL^{-1}$) for 1 h in the presence or absence of SB431542 (10 μM), which was added 1 h before ligand stimulation. SIS3 at a concentration of 5 μM was added 1 h before the ac.PMV stimulation.

Fluorescent labeling of PMVs

To analyze the adhesion of PMVs to EPCs, PMVs were labeled with PKH26, a general marker of the cell membrane (PKH26 Fluorescent Cell Linker Kits; MilliporeSigma, Billerica, MA, USA), and then incubated with EPCs for 0 min, 15 min, 30 min, 60 min, 3 h, 6 h, 12 h, or 24 h. The samples were fixed with 4% paraformaldehyde for 20 min and then washed three times with PBS. Then, DAPI diluted with PBS (1 : 1000) was added and incubated for 15 min. After three rinses, images were acquired by confocal microscopy (LV1000; Olympus).

Immunofluorescence staining and HE staining

Stimulated EPCs were fixed with 4% paraformaldehyde for 20 min, permeabilized with 0.1% Triton X-100 for 5 min, and immersed in a solution of 10% goat serum for 30 min at room temperature to block nonspecific binding. Subsequently, the cells were probed with the primary antibodies against Smad3, which were diluted with 10% goat serum (1 : 200) at 4 °C overnight. After washing, the cells were incubated with secondary antibody for 2 h, and then, DAPI was used for cell nuclei staining for 15 min at room temperature.

Hematoxylin and eosin staining was used for HE staining. Briefly, frozen sections were washed with tap water for 30 s, stained with hematoxylin, and lyophilized for 5 min. The sections were washed with water for 30 s and 1% hydrochloric acid in ethanol for 5 s. The sections were rinsed for 30 s and treated with reverse blue solution for 5 min. After washing for 30 s in tap water, the sections were stained with eosin staining solution for 30 min. They were treated with 80% ethanol for 1 min, treated with 95%

ethanol for 1 min, treated with absolute ethanol for 1 min, and cleared with xylene 3 times for 1 min each. The sections were sealed with neutral resin and observed under a microscope.

The frozen sections were placed in a dyeing tank, washed three times with PBS, and permeablized with 0.3% Triton X-100 for 30 min. The next steps were the same as those used in the cell experiments. Primary antibodies against vWF (Cell Signaling Technology, Danvers, MA, USA), CD41, and CD34 (an EPC maker; Santa Cruz Biotechnology, Dallas, TX, USA) were diluted 1 : 200 with 10% goat serum. Photographs were taken by confocal microscopy (LV1000; Olympus).

Quantitative real-time PCR

Total RNA was isolated with TRIzol Reagent. The isolated RNA was reverse transcribed into cDNA using reverse transcription primers for various mRNAs and oligo-dT for mRNA. mRNA expression was analyzed relative to glyceraldehyde 3-phosphate dehydrogenase (GAPDH) using SYBR Green Supermix (TaKaRa, Foster, CA, USA), and PCR product specificity was verified via melt curve analysis. The PCR conditions used for mRNA expression analysis were as follows: 95 °C for 30 s followed by 40 cycles of 95 °C for 5 s and 60 °C for 45 s. All primers used for quantitative RT-PCR analysis are listed in Table 1. Relative expression of the different genes was measured by the $2^{-\Delta\Delta Ct}$ method. The methods have also been described previously [52].

Western blot analysis

Western blot analysis was performed with antibodies against Smad3 (1 : 1000; Cell Signaling Technology), p-Smad3 (1 : 1000; Cell Signaling Technology), TGF-β1 (1 : 500; Bioss, Beijing, China), and GAPDH (1 : 5000; Proteintech, Chicago, IL, USA). After incubation with alkaline phosphatase-conjugated secondary antibodies (1 : 1000; Jackson ImmunoResearch Laboratories, West Grove, PA, USA), the signals were visualized with nitroblue tetrazolium/bromo-chloro-indolyl phosphate (Bio Basic, Markham, ON, Canada) and quantified with Image Studio.

Table 1. Sequences of primers.

Primer sequences (5′–3′)	
IL-2	F: GCACTGACGCTTGTCCTCCTTG
	R: GGAGCACCTGTAAGTCCAGCAAC
MMP9	F: CTACACGGAGCATGGCAACGG
	R: TGGTGCAGGCAGAGTAGGAGTG
TNC	F: AGCAGACTGGAGGAACTGGAGATG
	R: TTCACAGACACAGCCACAACCTTC
PDGFB	F: TCTCTGCTGCTACCTGCGTCTG
	R: AAGGAGCGGATGGAGTGGTCAC
TGF-β1	F: GGCACCATCCATGACATGAACCG
	R: GCCGTACGCAGCAGTTCTTCTCTG
CDKN1A	F: TGATATGTACCAGCCACAGG
	R: AACAGACGACGGCATACTTT
CDKN2A	F: CAGCTCTCCTGCTCTCCTATGGTG
	R: CAGGCATCGCGCACATCCAG
GAPDH	F: GGCACAGTCAAGGCTGAGAAT
	R: ATGGTGGTGAAGACGCCAGTA

Cell proliferation assay

Endothelial progenitor cells proliferation was analyzed *in vivo* using the *In Situ* Cell Proliferation Kit (Fluos; Roche, Basel, Switzerland). Twenty-four hours before harvest, BrdU was intraperitoneally injected into the rats (200 mg·kg^{-1}). Pieces of arteries (0.5 cm long) were isolated, fixed, dehydrated with isopentane for 24 h, fixed with 70% ethanol in 50 mM glycine buffer, digested with 0.05% trypsin solution, denatured with 2 M HCl, and labeled with an anti-BrdU antibody (1: 200). The nuclei were stained with DAPI in the next day. Blood vessels were dissected longitudinally and flattened between coverslips. Then, an FV1000 laser scanning confocal microscope (Olympus) was used to visualize EPC proliferation. The percentage of BrdU-positive cells to CM-Dil-positive cells was calculated.

Endothelial progenitor cells proliferation *in vitro* was analyzed with a colorimetric BrdU kit (Roche). Eight hours before the detection, BrdU labeling reagent was added to the culture medium (1 : 1000). EPCs were then fixed and labeled according to the manufacturer's instructions. Absorbance was measured at a wavelength of 450 nm and a reference wavelength of 630 nm with an ELISA plate reader (680; Bio-Rad, Hercules, CA, USA).

ELISA

The concentration of TGF-β1 in PMVs or ac.PMVs was determined by ELISA using a rat TGF-β1 ELISA kit (Neobioscience, Shenzhen, China). The assay was performed following the manufacturer's instructions.

Statistical analysis

Data from at least four independent experiments were analyzed, and all values are expressed as the mean ± SD. Student's *t*-test was used for two-sample comparisons. *P*-values < 0.05 were considered statistically significant.

Acknowledgements

This study was supported by grants from the National Natural Science Foundation of China (Nos. 11572198 and 11625209) and the Interdisciplinary Program of Shanghai Jiao Tong University (No. YG2017QN23).

Conflict of interest

The authors declare no conflicts of interest.

Author contributions

JY and YH designed the research; JY, HB, and YJF performed the research; ZLJ, YXQ, and YH contributed reagents or other essential material; JY analyzed data and wrote the paper; and JY and YH revised the manuscript.

References

1 Asahara T, Murohara T, Sullivan A, Silver M, van der Zee R, Li T, Witzenbichler B, Schatteman G & Isner JM (1997) Isolation of putative progenitor endothelial cells for angiogenesis. *Science* **275**, 964–966.

2 Nikos Werner MD, Sonja Kosiol MD, Tobias Schiegl MD, Patrick Ahlers MD, Katrin Walenta MD, Andreas Link MD, Michael Böhm MD & Georg Nickenig MD (2005) Circulating endothelial progenitor cells and cardiovascular outcomes. *N Engl J Med* **353**, 99–1007.

3 Gehling UM, Ergün S, Schumacher U, Wagener C, Pantel K, Otte M, Schuch G, Schafhausen P, Mende T, Kilic N *et al.* (2000) *In vitro* differentiation of endothelial cells from AC133-positive progenitor cells. *Blood* **95**, 3106–3112.

4 Gunsilius E, Duba HC, Petzer AL, Kähler CM & Gastl GA (2001) Contribution of endothelial cells of hematopoietic origin to blood vessel formation. *Circ Res* **88**, E1.

5 António N, Fernandes R, Soares A, Soares F, Lopes A, Carvalheiro T, Paiva A, Pêgo GM, Providência LA, Gonçalves L *et al.* (2014) Reduced levels of circulating endothelial progenitor cells in acute myocardial infarction patients with diabetes or pre-diabetes: accompanying the glycemic continuum. *Cardiovasc Diabetol* **13**, 101.

6 Asahara T, Kawamoto A & Masuda H (2011) Concise review: circulating endothelial progenitor cells for vascular medicine. *Stem Cells* **29**, 1650–1655.

7 Hur J, Yoon CH, Kim HS, Choi JH, Kang HJ, Hwang KK, Oh BH, Lee MM & Park YB (2004) Characterization of two types of endothelial progenitor cells and their different contributions to neovasculogenesis. *Arterioscler Thromb Vasc Biol* **24**, 288–293.

8 Tesfamariam B (2016) Endothelial repair and regeneration following intimal injury. *Cardiovasc Transl Res* **9**, 91–101.

9 Boilard E, Nigrovic PA, Larabee K, Watts GF, Coblyn JS, Weinblatt ME, Massarotti EM, Remold-O'Donnell E, Farndale RW, Ware J *et al.* (2010) Platelets amplify inflammation in arthritis via collagen-dependent microparticle production. *Science* **327**, 580–583.

10 Buzas EI, György B, Nagy G, Falus A & Gay S (2014) Emerging role of extracellular vesicles in inflammatory diseases. *Nat Rev Rheumatol* **10**, 356–364.

11 Zaldivia MTK, McFadyen JD, Lim B, Wang X & Peter K (2017) Platelet-derived microvesicles in cardiovascular diseases. *Frontiers in Cardiovascular Medicine* **4**, 74.

12 Brill A, Dashevsky O, Rivo J, Gozal Y & Varon D (2005) Platelet-derived microparticles induce angiogenesis and stimulate post-ischemic revascularization. *Cardiovasc Res* **67**, 30–38.

13 Prokopi M, Pula G, Mayr U, Devue C, Gallagher J, Xiao Q, Boulanger CM, Westwood N, Urbich C, Willeit J *et al.* (2009) Proteomic analysis reveals presence of platelet microparticles in endothelial progenitor cell cultures. *Blood* **114**, 723–732.

14 Alexandru N, Andrei E, Dragan E & Georgescu A (2015) Interaction of platelets with endothelial progenitor cells in the experimental atherosclerosis: role of transplanted endothelial progenitor cells and platelet microparticles. *Biol Cell* **107**, 189–204.

15 Watabe T & Miyazono K (2009) Roles of TGF-β family signaling in stem cell renewal and differentiation. *Cell Res* **19**, 103–115.

16 Han F, Shu J, Wang S, Tang CE & Luo F (2019) Metformin inhibits the expression of biomarkers of fibrosis of EPCs *in vitro*. *Stem Cells Int* **2019**, 9019648.

17 Teng L, Peng S, Guo H, Liang H, Xu Z, Su Y & Gao L (2015) Conditioned media from human ovarian cancer endothelial progenitor cells induces ovarian cancer cell migration by activating epithelial-to-mesenchymal transition. *Cancer Gene Ther* **22**, 518–523.

18 Garg M, Kaur S, Banik A, Kumar V, Rastogi A, Sarin SK, Mukhopadhyay A & Trehanpati N (2017) Bone marrow endothelial progenitor cells activate hepatic stellate cells and aggravate carbon tetrachloride induced liver fibrosis in mice via paracrine factors. *Cell Prolif* **50**, e12355.

19 Jinnin M, Ihn H & Tamaki K (2006) Characterization of SIS3, a novel specific inhibitor of Smad3, and its effect on transforming growth factor-beta1-induced extracellular matrix expression. *Mol Pharmacol* **69**, 597–607.

20 Zeng Z, Xia L, Fan X, Ostriker AC, Yarovinsky T, Su M, Zhang Y, Peng X, Xie Y, Pi L *et al.* (2019) Platelet-derived miR-223 promotes a phenotypic switch in arterial injury repair. *J Clin Investig* **129**, 1372–1386.

21 Deanfield JE, Halcox JP & Rabelink TJ (2007) Endothelial function and dysfunction: testing and clinical relevance. *Circulation* **115**, 1285–1295.

22 Wegiel B, Gallo DJ, Raman KG, Karlsson JM, Ozanich B, Chin BY, Tzeng E, Ahmad S, Ahmed A, Baty CJ *et al.* (2010) Nitric oxide-dependent bone marrow progenitor mobilization by carbon monoxide

enhances endothelial repair after vascular injury. *Circulation* **121**, 537–548.
23 Xia WH, Yang Z, Xu SY, Chen L, Zhang XY, Li J, Liu X, Qiu YX, Shuai XT & Tao J (2012) Age-related decline in reendothelialization capacity of human endothelial progenitor cells is restored by shear stress. *Hypertension* **59**, 1225–1231.
24 George AL, Bangalore-Prakash P, Rajoria S, Suriano R, Shanmugam A, Mittelman A & Tiwari RK (2011) Endothelial progenitor cell biology in disease and tissue regeneration. *J Hematol Oncol* **4**, 24.
25 Briasoulis A, Tousoulis D, Antoniades C, Papageorgiou N & Stefanadis C (2011) The role of endothelial progenitor cells in vascular repair after arterial injury and atherosclerotic plaque development. *Cardiovas Ther* **29**, 125–139.
26 Cheng M, Guan X, Li H, Cui X, Zhang X, Li X, Jing X, Wu H & Avsar E (2013) Shear stress regulates late EPC differentiation via mechanosensitive molecule-mediated cytoskeletal rearrangement. *PLoS ONE* **8**, e67675.
27 Li L, Liu H, Xu C, Deng M, Song M, Yu X, Xu S & Zhao X (2017) VEGF promotes endothelial progenitor cell differentiation and vascular repair through connexin 43. *Stem Cell Res Ther* **8**, 237.
28 Son Y, Kwon SM & Cho JY (2019) CD276 (B7–H3) Maintains proliferation and regulates differentiation in angiogenic function in late endothelial progenitor cells. *Stem Cells* **37**, 382–394.
29 Melki I, Tessandier N, Zufferey A & Boilard E (2017) Platelet microvesicles in health and disease. *Platelets* **28**, 214–221.
30 Duchez AC, Boudreau LH, Naika GS, Bollinger J, Belleannée C, Cloutier N, Laffont B, Mendoza-Villarroel RE, Lévesque T, Rollet-Labelle E *et al.* (2015) Platelet microparticles are internalized in neutrophils via the concerted activity of 12-lipoxygenase and secreted phospholipase A2-IIA. *Proc Natl Acad Sci USA* **112**, E3564–E3573.
31 Ray DM, Spinelli SL, Pollock SJ, Murant TI, O'Brien JJ, Blumberg N, Francis CW, Taubman MB & Phipps RP (2008) Peroxisome proliferator-activated receptor γ and retinoid X receptor transcription factors are released from activated human platelets and shed in microparticles. *Thromb Haemost* **99**, 86–95.
32 Liang H, Yan X, Pan Y, Wang Y, Wang N, Li L, Liu Y, Chen X, Zhang CY, Gu H *et al.* (2015) MicroRNA-223 delivered by platelet-derived microvesicles promotes lung cancer cell invasion via targeting tumor suppressor EPB41L3. *Mol Cancer* **14**, 58.
33 Mause SF, Ritzel E, Liehn EA, Hristov M, Bidzhekov K, Müller-Newen G, Soehnlein O & Weber C (2010) Platelet microparticles enhance the vasoregenerative potential of angiogenic early outgrowth cells after vascular injury. *Circulation* **122**, 495–506.
34 Díez M, Musri MM, Ferrer E, Barberà JA & Peinado VI (2010) Endothelial progenitor cells undergo an endothelial-to-mesenchymal transition-like process mediated by TGFbetaRI. *Cardiovasc Res* **88**, 502–511.
35 Rich JN (2003) The role of transforming growth factor-beta in primary brain tumors. *Front Biosci* **8**, e245–e260.
36 Breier G, Blum S, Peli J, Groot M, Wild C, Risau W & Reichmann E (2002) Transforming growth factor-beta and Ras regulate the VEGF/VEGF-receptor system during tumor angiogenesis. *Int J Cancer* **97**, 142–148.
37 Viñals F & Pouysségur J (2001) Transforming growth factor beta1(TGF-beta1) promotes endothelial cell survival during *in vitro* angiogenesis via an autocrine mechanism implicating TGF-alpha signaling. *Mol Cell Biol* **21**, 7218–7230.
38 Evrard SM, d'Audigier C, Mauge L, Israël-Biet D, Guerin CL, Bieche I, Kovacic JC, Fischer AM, Gaussem P & Smadja DM (2012) The profibrotic cytokine transforming growth factor-β1 increases endothelial progenitor cell angiogenic properties. *J Thromb Haemost* **10**, 670–679.
39 Derynck R & Zhang YE (2003) Smad-dependent and Smad-independent pathways in TGF-beta family signalling. *Nature* **425**, 577–584.
40 Ramachandran A, Vizán P, Das D, Chakravarty P, Vogt J, Rogers KW, Müller P, Hinck AP, Sapkota GP & Hill CS (2018) TGF-β uses a novel mode of receptor activation to phosphorylate SMAD1/5 and induce epithelial-to-mesenchymal transition. *Elife* **7**, e31756.
41 Matsuyama S, Iwadate M, Kondo M, Saitoh M, Hanyu A, Shimizu K, Aburatani H, Mishima HK, Imamura T, Miyazono K *et al.* (2003) SB-431542 and Gleevec inhibit transforming growth factor-beta-induced proliferation of human osteosarcoma cells. *Can Res* **63**, 7791–7798.
42 Ai WJ, Li J, Lin SM, Li W, Liu CZ & Lv WM (2015) R-Smad signaling-mediated VEGF expression coordinately regulates endothelial cell differentiation of rat mesenchymal stem cells. *Stem Cells Dev* **24**, 1320–1331.
43 Zhang J, Li Y, Li H, Zhu B, Wang L, Guo B, Xiang L, Dong J, Liu M & Xiang G (2018) GDF11 improves angiogenic function of EPCs in diabetic limb ischemia. *Diabetes* **67**, 2084–2095.
44 Midwood KS, Hussenet T, Langlois B & Orend G (2011) Advances in tenascin-C biology. *Cell Mol Life Sci* **68**, 3175–3199.
45 Jones PL & Jones FS (2000) Tenascin-C in development and disease: gene regulation and cell function. *Matrix Biol* **19**, 581–596.
46 Gulbis JM, Kelman Z, Hurwitz J, O'Donnell M & Kuriyan J (1996) Structure of the C-terminal region of p21(WAF1/CIP1) complexed with human PCNA. *Cell* **87**, 297–306.

47 Rayess H, Wang MB & Srivatsan ES (2012) Cellular senescence and tumor suppressor gene p16. *Int J Cancer* **130**, 1715–1725.
48 Griese DP, Achatz S, Batzlsperger CA, Strauch UG, Grumbeck B, Weil J & Riegger GA (2003) Vascular gene delivery of anticoagulants by transplantation of retrovirally-transduced endothelial progenitor cells. *Cardiovasc Res* **58**, 469–477.
49 Jobst BJ, Riegger GA & Griese DP (2009) Endothelial cell seeding fails to prevent intimal hyperplasia following arterial injury in the rat carotid model. *Cardiovasc Drugs Ther* **23**, 343–353.
50 Chen YH, Lin SJ, Lin FY, Wu TC, Tsao CR, Huang PH, Liu PL, Chen YL & Chen JW (2007) High glucose impairs early and late endothelial progenitor cells by modifying nitric oxide- related but not oxidative stress-mediated mechanisms. *Diabetes* **56**, 1559–1568.
51 Li H, Zhang X, Guan X, Cui X, Wang Y, Chu H & Cheng M (2012) Advanced glycation end products impair the migration, adhesion and secretion potentials of late endothelial progenitor cells. *Cardiovasc Diabetol* **11**, 46.
52 Li N, Wang WB, Bao H, Shi Q, Jiang ZL, Qi YX & Han Y (2019) MicroRNA-129-1-3p regulates cyclic stretch-induced endothelial progenitor cell differentiation by targeting Runx2. *J Cell Biochem* **120**, 5256–5267.
53 Laffont B, Corduan A, Plé H, Duchez AC, Cloutier N, Boilard E & Provost P (2013) Activated platelets can deliver mRNA regulatory Ago2•microRNA complexes to endothelial cells via microparticles. *Blood* **122**, 253–261.
54 Szatanek R, Baj-Krzyworzeka M, Zimoch J, Lekka M, Siedlar M & Baran J (2017) The methods of choice for extracellular vesicles (EVs) characterization. *Int J Mol Sci* **18**, E1153.